

**Translating International Commitments to
Domestic Action:
Mercury Co-Benefits, Sustainable Development,
and Climate Policy in China**

by

Kathleen Mara Mulvaney

B.S., Pennsylvania State University (2012)

Submitted to the Institute for Data, Systems, and Society
in partial fulfillment of the requirements for the degree of

Master of Science in Technology Policy

at the

MASSACHUSETTS INSTITUTE OF TECHNOLOGY

June 2017

© Massachusetts Institute of Technology 2017. All rights reserved.

Author
Institute for Data, Systems, and Society
May 12, 2017

Certified by
Noelle E. Selin
Associate Prof. of Data, Systems, and Society and Atmospheric
Chemistry
Thesis Supervisor

Accepted by
Munther Dahleh
W.A. Coolidge Prof. of Electrical Engineering and Computer Science
Director, Institute for Data, Systems, and Society
Acting Director, Technology and Policy Program

Translating International Commitments to Domestic Action: Mercury Co-Benefits, Sustainable Development, and Climate Policy in China

by

Kathleen Mara Mulvaney

Submitted to the Institute for Data, Systems, and Society
on May 12, 2017, in partial fulfillment of the
requirements for the degree of
Master of Science in Technology Policy

Abstract

National commitments on the Paris Agreement on climate change interact with other global environment and sustainability objectives, such as the Minamata Convention on Mercury and the global Sustainable Development Goals. Understanding the interactions between climate change, air pollution, and sustainable development can help decision-makers identify more effective policies that can address environmental and economic goals simultaneously. To address environmental goals, I assess how mercury co-benefits (positive side effects that are peripheral to a policy's main goal) of a national climate policy in China could contribute to the country's commitments under the Minamata Convention. I examine climate policy scenarios in 2030 corresponding to various levels of carbon intensity reductions in addition to a business-as-usual scenario and an end-of-pipe control scenario that meets China's commitments under the Minamata Convention on Mercury. Economic analysis from a computable general equilibrium model of China's economy provides information on changes in economic activity resulting from the climate policy scenarios. Using the economic data from this model, I scale 2007 mercury emissions in a variety of sectors to 2030. I then use a global atmospheric transport model to project changes in mercury deposition at the regional scale in China for each policy scenario. I find that climate policy in China can provide mercury emissions and deposition co-benefits similar to end-of-pipe control policies that meet the country's Minamata Convention commitments. To address sustainable development goals, I investigate the use of the Inclusive Wealth Index for evaluating the sustainability of climate policy in China on the basis of produced capital, natural capital, and human capital at the provincial level. I find that most provinces in China exhibit an increase in Inclusive Wealth under several climate policy scenarios, providing an alternative metric for monetizing policy impacts.

Thesis Supervisor: Noelle E. Selin

Title: Associate Prof. of Data, Systems, and Society and Atmospheric Chemistry

Acknowledgments

My time at MIT has been a wild ride, and I never would have been able to navigate this place without the help of many people. First and foremost, thank you to my research advisor, Noelle Selin, for taking a risk and welcoming a mechanical engineer from the nuclear industry into your research group. Your guidance these past two years has been invaluable, and you've built quite an impressive team of people to back you up. To the Selin Group: your training, tough questions, and comradery helped build this thesis. Thank you especially to Amanda Giang, for your unyielding patience as a TA, help with GEOS-Chem, and encouragement; H el ene Angot for the hours of time you saved me talking through code issues and encouraging all of us to take a break for Fridays at the Muddy; Mingwei Li for your guidance on my first research project at MIT; Sae Yun Kwon for sharing your knowledge on mercury and your positivity; Colin Thackray and Daniel Rothenberg for teaching me two thirds of what I know about Python; and everyone else in the Selin Group. It has been a pleasure working with you.

Thank you also to Valerie Karplus and the Karplus Energy Group, formerly known as the China Energy and Climate Project, particularly Da Zhang and Chiao-Ting Li for educating me on C-REM, and Paul Kishimoto for teaching me the other one third of what I know about Python. It has been wonderful being part of not one, but two vibrant research groups.

TPP is the best collection of people at MIT. Thank you to Ed Ballo, Barb De-LaBarre, and Frank Field for everything you do for us, from helping us graduate on time to laughing with us in the TPP lounge. To the TPP lady gang: you have saved me the past two months. I don't know how I would have made it to the end of this adventure without your friendship. From the bottom of my heart, thank you for showing up to our study sessions and breaks when I most needed your company.

To Brandon: thank you for your love that helped me to grow.

And finally, thank you to Mom, Dad, and Connor. You guys are the root of my strength. I love you.

Contents

| | | |
|----------|--|-----------|
| 1 | Introduction | 13 |
| 1.1 | Motivation | 13 |
| 1.2 | Translating International Agreements to Domestic Action | 14 |
| 1.2.1 | International Governance on Climate Change | 14 |
| 1.2.2 | International Governance on Mercury Pollution | 15 |
| 1.2.3 | China’s Domestic Action on Climate Change and Mercury Pollution | 16 |
| 1.3 | Thesis Questions | 19 |
| 1.4 | Organization | 20 |
| 2 | Mercury Co-Benefits of Climate Policy in China | 21 |
| 2.1 | Background | 21 |
| 2.1.1 | Environmental Science of Mercury and Governance | 21 |
| 2.1.2 | Previous Work on Air Pollution Co-Benefits | 23 |
| 2.1.3 | Previous Work on Mercury Pollution and Policy | 23 |
| 2.2 | Methods | 30 |
| 2.2.1 | Base Emissions Inventory: EDGARv4.tox1 | 30 |
| 2.2.2 | Policy Scenarios | 30 |
| 2.2.3 | Projecting Emissions Without Considering APCDs | 33 |
| 2.2.4 | Projecting Emissions to Account for Future Changes in APCDs: Power Generation and Industry Combustion | 36 |
| 2.2.5 | Transport and Deposition | 38 |
| 2.3 | Results and Discussion | 42 |

| | | |
|----------|--|-----------|
| 2.3.1 | Emissions Projections to 2030 | 42 |
| 2.3.2 | Total Deposition in 2030 | 51 |
| 2.3.3 | Discussion | 57 |
| 2.4 | Policy Implications | 58 |
| 3 | Evaluating Policy for Sustainable Development in China | 61 |
| 3.1 | Background | 61 |
| 3.1.1 | History of Sustainable Development | 61 |
| 3.1.2 | The Inclusive Wealth Index (IWI) | 62 |
| 3.1.3 | Using IWI as a Tool for Policy Analysis | 63 |
| 3.2 | A Framework for Evaluating Climate Policy in China Using IWI . . . | 64 |
| 3.2.1 | Produced Capital | 64 |
| 3.2.2 | Natural Capital | 65 |
| 3.2.3 | Health Capital to Represent Human Capital | 66 |
| 3.2.4 | Results | 67 |
| 3.2.5 | Discussion | 67 |
| 3.2.6 | Options for Incorporating Mercury Pollution | 72 |
| 4 | Policy Recommendations and Conclusions | 75 |
| 4.1 | Taking Action on Climate Change and Meeting Environmental Goals Effectively | 75 |
| 4.2 | Sustainable Development and Meeting Environmental Goals Effectively | 76 |
| 4.3 | Incentive for Collective Action | 78 |

List of Figures

| | | |
|------|---|----|
| 2-1 | Chinese Provinces Evaluated by C-REM | 25 |
| 2-2 | 2050 Emissions Projection Results, Giang et al. (2015) | 28 |
| 2-3 | 2007 EDGAR Emissions, China (Muntean et al., 2014) | 37 |
| 2-4 | Total Mercury Emissions in China, 2030 Policy Scenarios | 44 |
| 2-5 | Relative Contribution by Sector to National Emission Reductions | 45 |
| 2-6 | Distribution of Total Emissions by Province, 2030 BAU Scenario | 46 |
| 2-7 | Speciated Emissions, 2030 BAU Scenario | 47 |
| 2-8 | Sector Emissions by Province, 2030 BAU Scenario | 48 |
| 2-9 | Distribution of Total Mercury Emissions in China | 49 |
| 2-10 | Relative Contribution of Emissions Reductions by Province | 50 |
| 2-11 | Wet and Dry Deposition, 2030 BAU Scenario | 52 |
| 2-12 | Distribution of Total Mercury Deposition in China | 53 |
| 2-13 | Global Total Deposition, 2030 BAU Scenario | 54 |
| 2-14 | Distribution of Global Total Deposition | 55 |
| 3-1 | United Nations Sustainable Development Goals | 62 |
| 3-2 | Change in Inclusive Wealth Index Compared to 2030 BAU Case | 68 |
| 3-3 | Changes in Produced Capital | 69 |
| 3-4 | Changes in Natural Capital | 70 |
| 3-5 | Changes in Health Capital | 71 |

List of Tables

| | | |
|------|--|----|
| 2.1 | Chinese Provinces Evaluated by C-REM | 24 |
| 2.2 | C-REM Sectors Used to Project Mercury Emissions | 25 |
| 2.3 | EDGARv4.tox1 Mercury Inventory Economic Sectors | 31 |
| 2.4 | EDGARv4.tox1 Power Generation and Industry Combustion Sub-Sectors | 31 |
| 2.5 | Policy Scenarios for Evaluating Mercury Co-Benefits of Climate Policy in China | 32 |
| 2.6 | EDGAR Sectors Projected Without Considering APCDs and Corre- sponding C-REM Sectors and Outputs for Scaling to 2030 | 34 |
| 2.7 | EDGAR Sectors Projected With Consideration of APCDs and Corre- sponding C-REM Sectors and Outputs for Scaling to 2030 | 36 |
| 2.8 | 2010 APCD Application and Mercury Capture Factors | 39 |
| 2.9 | 2030 Business-as-Usual APCD Application and Mercury Capture Factors | 40 |
| 2.10 | 2030 Business-as-Usual APCD Speciation Factors | 40 |
| 2.11 | 2030 Minamata Convention APCD Application and Mercury Capture Factors | 41 |
| 2.12 | 2030 Minamata Convention APCD Speciation Factors | 41 |
| 2.13 | China and the Global Mercury Budget | 56 |

Chapter 1

Introduction

Economic activity, climate change, and air pollution are intertwined. Industrial activity serves as the engine to develop an economy and lift people out of poverty while likely releasing carbon dioxide and a range of pollutants harmful to human health into the atmosphere. Developing solutions to grow economies sustainably while also addressing issues of climate change and air pollution present some of the most difficult political and technical challenges of our time. This thesis demonstrates how stakeholders can utilize tools to evaluate policy solutions that address these challenges simultaneously.

1.1 Motivation

International cooperation efforts from the United Nations that predate international environmental negotiations have long recognized the interaction between economic activity and environmental issues. The World Commission on Environment and Development (WCED, commonly known as the Brundtland Commission) released the report “Our Common Future” in 1987 providing a “global agenda for change” (WCED, 1987). The report highlights the effects of economic development on the environment and the ways in which environmental effects can inhibit development, from nuclear war started by developed countries to diminished soil quality resulting from poor agricultural practices in developing countries. Parties to global negotiations followed the lead of the Brundtland Commission and incorporated principles of sustainable development into the text of environmental agreements in subsequent years. Three major environmental agreements identify principles of sustainable development in their preambles, including the Montreal Protocol on Substances that Deplete the Ozone Layer (entered into force in 1989), the Minamata Convention on Mercury (agreed in 2013), and the Paris Agreement on climate change (agreed 2015) (UNEP, 2016a, 2013a; UNFCCC, 2015).

Concerted efforts at the international level are important to encourage domestic action on issues of the environment and sustainable development. However, the structure of the Paris Agreement on climate change and the Minamata Convention on Mercury rely heavily on national level action, which presents its own set of chal-

lenges. The complexity of these two international environmental agreements reflects the unique situations of each country party with a different set of priorities at the domestic level. Taking a holistic view of a country's priorities and commitments under international agreements can potentially reveal a set of policy options that minimize disadvantageous tradeoffs across environmental action and economic development while efficiently addressing multiple problems through utilizing "co-benefits".

I will use the term **co-benefits** throughout this thesis, referring to **positive side effects of policies that are peripheral to a policy's main goal**.

1.2 Translating International Agreements to Domestic Action

To illustrate the complexity of translating international commitments to national action, I will describe the development of the Paris Agreement and Minamata Convention, as well as China's evolving domestic action on climate change and mercury pollution.

1.2.1 International Governance on Climate Change

The hallmark Paris Agreement on climate change, a legally binding treaty negotiated under the United Nations Framework Convention on Climate Change (UNFCCC), was agreed in December 2015 and entered into force in November 2016 (United Nations, 2016). Described as a "Climate Revolution for All" by the Earth Negotiations Bulletin, the globally inclusive agreement was the result of 25 years of research and negotiation (IISD, 2015).

In November 1990, the international scientific body charged by the World Meteorological Organization (WMO) and the United Nations Environment Programme (UNEP) with assessing global climate change, the Intergovernmental Panel on Climate Change (IPCC), released its First Assessment Report. The report concluded that anthropogenic emissions result in a higher concentration of greenhouse gases in Earth's atmosphere (Houghton et al., 1990). With each subsequent Assessment Report, the IPCC has stated with increasing confidence (statistically speaking) that anthropogenic greenhouse gases have an effect on the planet, namely on climate change and rising global temperatures. The latest IPCC position, from the Fifth Assessment Report, states that the effect of exceptional levels of anthropogenic greenhouse gas emissions "... together with those of other anthropogenic drivers, have been detected throughout the climate system and are extremely likely to have been the dominant cause of the observed [global] warming since the mid-20th century" (Pachauri et al., 2014).

The Paris Agreement is the second legally binding instrument (following the Kyoto Protocol) negotiated under the umbrella UNFCCC treaty in the institution's 25 year lifespan (UNFCCC, 1992, 1998). As of May 2017, 144 parties out of 197 member countries had ratified the Paris Agreement (UNFCCC, 2017). It utilizes three main policy instruments to address climate change, including mitigation, adaptation, and

finance on a schedule of five-year review cycles (IISD, 2015). Parties are legally bound to submit a Nationally Determined Contribution (NDC) every five years in the spirit of the “transparency framework” set up by the agreement (IISD, 2015; UNFCCC, 2015). Additionally, parties are committed to participating in a global stocktake every five years to evaluate progress toward meeting the goals of the agreement, including capping global temperature rise at 2 degrees Celsius (UNFCCC, 2015).

However, parties are not legally bound to complete the plans set out in the NDCs, which detail mitigation efforts to reduce greenhouse gas emissions, plans for adapting to the effects of climate change, financial requirements (for developing countries) or contributions (for developed countries) for implementing the NDCs, and capacity-building efforts to create institutions that aid in implementing the NDCs (IISD, 2015; UNFCCC, 2015). These policy instruments essentially utilize a pledge-and-review process, where parties pledge their mitigation, adaptation, and financial contributions through the NDCs, and then review their efforts every five years with the global stocktake initiative.

The pledge-and-review approach is an attractive strategy for carbon mitigation and climate action because it is politically feasible and implementable in its vagueness. It allows countries to create plans for climate action tailored to their unique situation that are theoretically implementable and can change over time. This feature is important to achieving a globally inclusive agreement that can motivate all countries to act toward a common goal of keeping global temperature rise below 2 degrees Celsius, especially since the parties to the Paris agreement do not quite achieve this benchmark. Analyses performed by the nonprofit Climate Interactive show that the NDCs submitted as of April 2016 could lead to a global temperature rise of approximately 3.5 degrees Celsius (Sterman et al., 2013; Climate Interactive, 2017).

1.2.2 International Governance on Mercury Pollution

Mercury has been used in a wide range applications throughout human history, from medicines and consumer products to mining processes, which translates to a long history of release to the environment (Selin, 2014). The element is also emitted as a by-product from industrial processes like coal combustion and metals processing (Selin, 2014). Mercury in the atmosphere exists in three forms with distinct transport characteristics. Elemental mercury, Hg^0 , has the longest lifetime of the three species and is susceptible to long range transport. Divalent mercury and particulate-bound mercury, Hg^{2+} and HgP , have a much shorter lifetime and are deposited nearby the source. Mercury pollution thus presents both an international and local environmental problem.

Mercury’s global biogeochemical cycle combined with neurologic health effects of childhood and in-utero exposure, as well as cardiovascular health effects of adulthood exposure have motivated the international community to negotiate a treaty to limit the impact of mercury on the environment (Yorifuji et al., 2013; Giang & Selin, 2016). UNEP called for the first global mercury assessment in 2001 in response to a request by the United States (Selin, 2014). Following 12 years of voluntary initiatives to decrease mercury releases and emissions, the Minamata Convention on Mercury was

adopted in October 2013 by 91 country parties to the convention, and as of May 2017, 43 parties had ratified the convention (IISD, 2013; UNEP, 2017; Selin, 2014).

The Minamata Convention addresses mercury pollution in its various chemical forms and environmental exposure pathways. It tackles the issue of mercury releases from both commercial products and industrial processes by phasing out and phasing down the direct use of mercury where possible as well as controlling and reducing by-product mercury emissions (UNEP, 2013a,b; IISD, 2013). The treaty utilizes a mix of trade restrictions, strict phase-out and phase-down schedules for the use of mercury in products and processes, and flexible compliance mechanisms that are similar to the Paris Agreement (Selin, 2014). The Convention directs Parties to create a National Implementation Plan to control emissions from new sources using best available techniques and best environmental practices as well as existing sources and submit it to the Conference of the Parties within four years of the treaty’s entry into force. Specifically, National Implementation Plans must implement at least one measure listed in the Convention to control mercury emissions from existing sources, which includes “a multi-pollutant strategy that would deliver co-benefits for control of mercury emissions,” (UNEP, 2013a).

While some requirements of the Minamata Convention involve legally binding restrictions on specific sources of mercury, parties to the Minamata Convention are not bound to an explicit target for reducing emissions from new and existing emissions sources, similar to the pledge-and-review approach of the Paris Agreement (UNEP, 2013a). Additionally, Lin et al. (2017) argue that the mix of strict and flexible implementation requirements could lead to releases of mercury from interconnected sources that are not covered by the Minamata Convention.

Like the Paris Agreement, the assortment of policy instruments utilized in the Minamata Convention reflects the complex behavior of the mercury biogeochemical cycle combined with the wide array of national circumstances of country parties. Overall, the design of the Minamata Convention allows for politically feasible action on mercury pollution.

1.2.3 China’s Domestic Action on Climate Change and Mercury Pollution

While the Paris Agreement and Minamata Convention on Mercury are impressive feats of international cooperation, another challenge comes when implementing the agreements at the national level. International environmental negotiations are a two-level game, as described by Robert Putnam (Putnam, 1988). The main idea of the two-level game concept is that domestic policy and international affairs are “entangled”. Putnam says there are two levels to the game of international negotiations. Level I involves negotiating that happens at the international level among the parties to the Paris Agreement and Minamata Convention, where the ultimate goal is to come to a global agreement. Level II involves negotiating that happens within each country at the domestic level in order to accept and implement the agreements.

Furthermore, at the national level, countries often do not act as unified “national

actors” according to Graham Allison’s Bureaucratic Politics Paradigm (Allison, 1969). Allison says governments can instead act as a “loose alliance of semi-independent organizations.” Under this paradigm, a policy outcome is the result of “compromise, coalition, competition, and confusion” among the independent organizations and goals of a government. Through this lens, it is clear that flexible, pledge-and-review approaches to environmental treaties can be considered politically feasible because they allow for the compromises, coalition, competition, and confusion that are inevitable to occur within the bounds of complex human and Earth systems.

China is no exception to the two-level game and bureaucratic politics paradigm. In their case, “compromise, coalition, competition, and confusion” has occurred between the country’s environmental goals and sustainable development goals and created some complications in the country’s negotiating position on international environmental governance. Starting with China’s action on climate change, Hilton & Kerr (2017) provide an overview of the country’s domestic climate action, economic development, and international negotiating positions in the years leading up to the Paris agreement. China began climate-related measures on energy efficiency and energy intensity reduction targets (the amount of energy produced per unit of GDP) in 2004. In 2005, the country passed the Renewable Energy Law that stimulated the growth of renewable energy in the country while also improving the overall energy system by advancing energy supplies, structure, and security in addition to addressing both environmental and economic development goals (Hilton & Kerr, 2017; Schuman & Lin, 2012). Also in 2005, the Eleventh Five-Year Plan was released with goals to reduce energy intensity and environmental pollutants (Kai, 2006). In 2007, China established a national office on climate change (Hilton & Kerr, 2017). In 2009, China’s negotiating stance was obstinate that international commitments to mitigate climate change should not interfere with economic development, effectively contributing to a block of a comprehensive agreement at the Copenhagen Climate Conference (Hilton & Kerr, 2017).

The tone of China’s negotiating position changed at the Paris Climate Conference in 2015, however, as the country’s economic situation and environmental goals aligned to create a more friendly atmosphere for cooperating on global climate action. On the domestic level, President Xi Jinping and Premier Li Keqiang introduced goals to slow economic growth and improve environmental pollution in 2013-2015 (Hilton & Kerr, 2017). China submitted their Intended NDC (INDC) to the UNFCCC (which has since become their first NDC to the Paris Agreement), communicating their goal to reduce energy intensity and peak their carbon dioxide emissions by 2030 (NDRC, 2015). The tone of the NDC expresses China’s recognition that action on climate change “requires collaboration of the international community”, in stark contrast to their position at Copenhagen (NDRC, 2015).

How will China achieve the pledges outlined in its NDC? One strategy the country may use is a cap and trade system that would ultimately decarbonize the country’s economy and reduce the energy intensity of the country’s most resource intensive industries. A cap-and-trade program serves to internalize environmental externalities by essentially assigning the right to pollute through a pricing system. Climate change can be considered an environmental externality in addition to a collective action

problem. An externality occurs in a market when the price of an action for a consumer or a firm is not equal to the social cost of that action, resulting in private benefits that do not equal social benefits (Kerr, 2015a). One remedy for externalities in a market is to find a way to “internalize” them (Ellerman et al., 2003). Emissions trading internalizes the environmental externalities of climate change by placing a price on carbon emissions that theoretically matches its social cost (Ellerman et al., 2003). A cap-and-trade approach involves setting a cap on total emissions (for a certain division of a country, a whole country, or the world), creating permits for emitting carbon, and allowing those permits to be bought and sold by firms in a market (Ellerman et al., 2003).

In 2015, China announced their plan to launch a national cap-and-trade program by 2017, although the country has yet to announce the launch so far this year (Davis & Davenport, 2015). In support of this effort, China’s National Development and Reform Commission (NDRC) launched seven pilot cap-and-trade programs in 2011 in cities and provinces across the country, including Beijing, Chongqing, Shanghai, Shenzhen, Tianjin, Guangdong, and Hubei (Munnings et al., 2014). A report by Resources for the Future published in 2014 concluded that emissions permit prices for the pilot programs were relatively stable through 2014, but the pilot programs have some issues related to compliance, cap setting, and carrying through the cost of emissions trading to consumers (Munnings et al., 2014). The pilot programs will be the basis for the national cap-and-trade program to be implemented as part of the Thirteenth Five-Year Plan, 2016-2020 (Swartz, 2016).

Similar to the issue of international action on climate change, China’s negotiating stance on global mercury pollution has changed over time, as discussed by Stokes et al. (2016). During UNEP’s initial efforts to organize global action on mercury in the early 2000s, China made the case that developing countries in their position were not able to take action on mercury pollution due to unfamiliarity with the problem. They also argued that a global treaty specific to mercury was not necessary in the first place given voluntary initiatives (Stokes et al., 2016). In the following years, China teamed up with India to resist a global treaty on mercury, reflecting national priorities dedicated to economic development through the expanded use of fossil fuels (Stokes et al., 2016). However, in 2013, China’s negotiating position diverged from India and shifted to support international governance of mercury through national implementation plans that address emissions control, mirroring the change they would make in their stance on global climate action a few years later (Stokes et al., 2016).

China is already taking steps to meet its commitments under the Minamata Convention on Mercury, which they ratified on August 31, 2016 (UNEP, 2017). Prior to ratification, China initiated a project in July 2015 with the World Bank to identify implementation plans at the national and provincial level, and also to build the country’s capacity to support implementation (World Bank, 2015). As part of developing a national strategy, the World Bank project will identify industrial sector-level actions, including those related to coal fired power plants, coal fired industrial boilers, municipal and medical waste, cement production, and non-ferrous metals production (World Bank, 2016). The project identifies that mercury action plans will be “integrated in multi-pollutant control texts and provisions,” (World Bank, 2016). However,

the project specifically does not investigate synergies with climate change adaptation and mitigation in China (World Bank, 2016).

1.3 Thesis Questions

The pledge-and-review approach of the Paris Agreement and National Implementation Plan approach of the Minamata Convention illustrate the magnitude of the collective action challenge associated with global action on climate change and mercury pollution. Climate change and mercury pollution are collective action problems that do not respect country boundaries. They affect the whole globe, a very large group that has little incentive to act. According to Mancur Olson, a collective action problem can be characterized as follows, “Since any gain goes to everyone in the group, those who contribute nothing to the effort will get just as much as those who made a contribution. It pays to ‘let George do it,’ but George has little or no incentive to do anything in the group interest either, so . . . there will be little, if any, group action,” (Olson, 1982). However, air pollution problems such as mercury, as well as economic development, have a local component. Policy options that address local issues and international problems simultaneously could provide greater incentive to address collective action problems.

The concept of taking concerted efforts to address multiple environmental and economic issues at once through policies that maximize co-benefits is not new. Working Group III of the Intergovernmental Panel on Climate Change addressed potential response strategies in the very first assessment report of the IPCC, published in 1990 (IPCC, 1990). They noted that the best options for responding to climate change holistically address a range of social, economic, and environmental issues while also being aligned with sustainable development (IPCC, 1990). More specifically, they highlight mitigation strategies such as improved energy efficiency and use of clean energy sources that decrease a variety of pollutants in addition to reducing carbon dioxide emissions. Many researchers have taken steps to quantify the suggestions set forth by the IPCC, evaluating air pollution reductions from future climate change mitigation strategies globally, nationally, and locally (for example, Cifuentes et al. (2001); West et al. (2006); Thompson et al. (2014); Silva et al. (2016)).

In this thesis, I demonstrate how integrated assessment and new economic indicators could help the global community and individual countries explore opportunities for coordination across national policies that take advantage of localized co-benefits, minimize disadvantageous tradeoffs across environmental action and economic development, and take steps toward global collective action.

I focus on China for my analyses. China’s Thirteenth Five Year Plan, detailed in the 2016 Report on the Work of the Government, identifies a commitment to development as a top priority for success of the plan, as well as placing an emphasis on measures to control air pollution throughout the country (Keqiang, 2016). However, as a government focused on central planning, China may not yet consider local-level effects of national policies that create winners and losers. Additionally, China is the world’s highest emitter of carbon dioxide and mercury (Li et al., 2017b; Zhang

et al., 2015). The country is at the beginning of the policymaking process for climate and environmental policy under the Paris Agreement and Minamata Convention on Mercury, and it is poised to take the lead on international climate governance in the coming years.

I explore the interactions between climate change, air pollution (focusing on mercury emissions), and sustainable development in China by addressing the following questions.

1. How do mercury co-benefits of climate policy in China contribute to the country's commitments under the Minamata Convention on Mercury, from the national level to the regional level?
2. How can China evaluate the contribution of climate policy to their sustainable development goals, from the national level to the regional level?
3. How can decision-makers consider the interacting factors of climate change, air pollution, and economic development in evaluating regional effects of national-level policy options that address international commitments to take action on climate change, meet environmental goals effectively, and develop sustainably?

1.4 Organization

Chapter 2 presents an analysis on the mercury emissions and deposition co-benefits of climate policy in China, addressing the first research question. Chapter 3 introduces a framework for evaluating climate policy options in China for sustainability at the province level using the Inclusive Wealth Index, addressing the second research question. Chapter 4 presents policy recommendations and conclusions to address the third research question.

Chapter 2

Mercury Co-Benefits of Climate Policy in China

Mercury is emitted from both natural and anthropogenic sources into the atmosphere, with about 30 percent coming from current-day anthropogenic sources, 10 percent from natural geologic sources, and 60 percent from legacy sources that result from cycling between land, the ocean, and the atmosphere (Muntean et al., 2014). Anthropogenic sources include combustion activities for heat and power generation, industrial processes, large and small scale gold mining, and waste incineration (Muntean et al., 2014). Mercury emissions from combustion activities are directly linked to carbon emissions affecting climate change, and mercury emissions from industrial processes that have some kind of carbon footprint are also indirectly linked to climate change. Decarbonization that slows economic growth may manifest as reduced production from those industries, and thus, reduced mercury emissions, presenting potential co-benefits of climate policy (Li et al., 2017b).

In this chapter, I present an analysis of the mercury emissions and deposition co-benefits of decarbonizing China's economy through a national climate policy, examining the results on varying spatial scales.

2.1 Background

Here I discuss the science of the mercury biogeochemical cycle, China's involvement in the Minamata Convention, and previous work on air pollution co-benefits of climate policy.

2.1.1 Environmental Science of Mercury and Governance

Several characteristics make mercury a unique metal, including its liquid state at standard conditions and its gaseous state in the atmosphere (Ariya et al., 2015; Jacob, 2016). In the atmosphere, elemental mercury, Hg^0 , can shed two electrons and be reduced to divalent mercury, Hg^{2+} , which reacts with other species in the atmosphere or adsorbs onto the surface of aerosol particles to form HgP (Ariya et al., 2015; Subir

et al., 2012). Mercury is primarily emitted from anthropogenic sources as Hg^0 , but combustion processes also emit Hg^{2+} and HgP (Driscoll et al., 2013). These three species of mercury have distinct redox chemistry and transport characteristics.

Mercury speciation dictates its lifetime and as a result transport in the atmosphere. Pollutants are transported on a time scale of weeks to months within a hemisphere and a time scale of one year between hemispheres (Jacob, 1999). Hg^0 is susceptible to global transport with a lifetime of 6 months to one year (Driscoll et al., 2013). Hg^{2+} and HgP are both water-soluble and susceptible to wet and dry deposition, leading to a lifetime on the order of days to weeks (Selin, 2009). As a result, Hg^{2+} and HgP do not travel as far as Hg^0 and are considered local pollutants. Once emitted, mercury can cycle through terrestrial, ocean, and atmospheric systems for thousands to tens of thousands of years before reaching a final resting place in deep ocean reservoirs (Selin, 2009; Amos et al., 2013).

The Minamata Convention addresses mercury pollution in its various chemical forms and environmental exposure pathways. It addresses the issue of mercury releases from both commercial products and industrial processes by phasing out and phasing down the direct use of mercury where possible as well as controlling and reducing by-product mercury emissions (UNEP, 2013b; IISD, 2013; UNEP, 2013a). UNEP defines by-product emissions as mercury released from fuels and raw materials that contain mercury as an impurity (UNEP, 2013b). Activities exhibiting by-product mercury emissions include coal burning, mining, metals production processes involving ores, and raw materials processing to produce cement (UNEP, 2013b). Here, I focus on mercury by-product emissions potentially affected by decarbonizing China's economy through a national climate policy.

China will be a major contributor to the Minamata Convention on Mercury based on several analyses conducted to project mercury emissions. Streets et al. (2009) project global mercury emissions to 2050 and find that emissions in Asia, especially from coal-fired power plants, are a significant driver of future emissions. Similarly, Rafaj et al. (2013) find that China emissions could comprise around 38 percent of world mercury emissions by 2050 in their baseline scenario.

In this study, I evaluate near-term mercury co-benefits of climate policy by examining emissions, transport, and deposition under future policy scenarios in 2030, examining results at the global level, as well as the national and regional level in China. I compare emissions and deposition benefits across a business-as-usual policy scenario, end-of-pipe control policy scenario that meets China's commitments under the Minamata Convention, and three different climate policy scenarios of varying stringency. I project the Emissions Database for Atmospheric Research (EDGAR) 2007 mercury emissions inventory over China from Muntean et al. (2014) to 2030 using economic output data with province-level detail from the China Regional Energy Model (C-REM), a computable general equilibrium model utilized by Li et al. (2017a). I then evaluate the transport of 2030 mercury emissions and resulting deposition in China and the rest of the world using a global chemical transport model, drawing on the methods utilized by Giang et al. (2015).

2.1.2 Previous Work on Air Pollution Co-Benefits

Air Pollution Co-Benefits in China

At the national level in China, several researchers have evaluated the air pollution co-benefits of climate policy with the aid of computable general equilibrium (CGE) models to characterize emissions. CGE models rely on the economic concept of general equilibrium, in which supply equals demand in all sectors within an economy, taking into account the availability of resources, consumer preference of a given good to be substituted for another, changes in consumer income, and changes in prices (Kerr, 2015c). CGE models are powerful tools because they can capture the interconnectedness of sectors and sub-economies in a given country (Kerr, 2015c). This is important for China because interprovincial trade and differing levels of economic development between coastal provinces and the central and western provinces are hallmarks of the country's economy (Springmann et al., 2015).

In this study, I utilize the CGE model results from Li et al. (2017b) to project mercury emissions to 2030 under climate policy in China. Li et al. (2017b) utilize a CGE model (the China Regional Energy Model, C-REM) to evaluate the particulate matter (PM_{2.5}) co-benefits of climate policy in China in 2030. C-REM models China's economy at the provincial level, capturing economic interactions amongst provinces as well as between China and the rest of the world (Springmann et al., 2015; Zhang et al., 2016a, 2013). I use the C-REM model results from Li et al. (2017b) to project the 2007 EDGAR emissions from China to 2030. C-REM outputs economic data for the 30 provinces in China listed in Table 2.1 and shown in Figure 2-1 under prescribed policy perturbations (Springmann et al., 2015; Zhang et al., 2013, 2016a). Economic data include GDP, energy use, sectoral outputs, carbon dioxide (CO₂) emissions, and sulfur dioxide (SO₂) by economic sector. The sectors included in C-REM are based on the 2007 edition of the Global Trade Analysis Project (GTAP) database (Springmann et al., 2015; Zhang et al., 2013, 2016a). The C-REM sectors relevant to this analysis are described in Table 2.2.

Several other groups of researchers have utilized a CGE model of China to evaluate air pollution co-benefits studies, although no one has examined mercury. Li et al. (2017b) explains these studies in detail, but I provide a summary here for information. Nielsen & Ho (2013) evaluate the impact of a carbon tax on SO₂, nitrogen oxides (NO_x), ozone, and PM_{2.5} in 2020 using an integrated assessment framework including a single-country CGE model of China that captures provincial-level interactions. Nam et al. (2013) examine national-level CO₂ co-benefits of SO₂ and NO_x regulations in China using a global CGE model. Finally, Dong et al. (2015) use a global CGE model with province-level detail of China in order to evaluate SO₂, NO_x, and PM_{2.5} under a variety of scenarios that include end-of-pipe air pollution controls and a cap on carbon.

2.1.3 Previous Work on Mercury Pollution and Policy

Evaluating mercury pollution on the basis of policy typically involves two steps: first, compiling an emissions inventory under a given time period or future policy scenario,

Table 2.1: Chinese Provinces Evaluated by C-REM

| Province | Abbreviation |
|-----------------|---------------------|
| Anhui | (AH) |
| Beijing | (BJ) |
| Chongqing | (CQ) |
| Fujian | (FJ) |
| Guangdong | (GD) |
| Gansu | (GS) |
| Guangxi | (GX) |
| Guizhou | (GZ) |
| Henan | (HA) |
| Hubei | (HB) |
| Hebei | (HE) |
| Hainan | (HI) |
| Heilongjiang | (HL) |
| Hunan | (HN) |
| Jilin | (JL) |
| Jiangsu | (JS) |
| Jiangxi | (JX) |
| Liaoning | (LN) |
| Inner Mongolia | (NM) |
| Ningxia | (NX) |
| Qinghai | (QH) |
| Sichuan | (SC) |
| Shandong | (SD) |
| Shanghai | (SH) |
| Shaanxi | (SN) |
| Shanxi | (SX) |
| Tianjin | (TJ) |
| Xinjiang | (XJ) |
| Yunnan | (YN) |
| Zhejiang | (ZJ) |

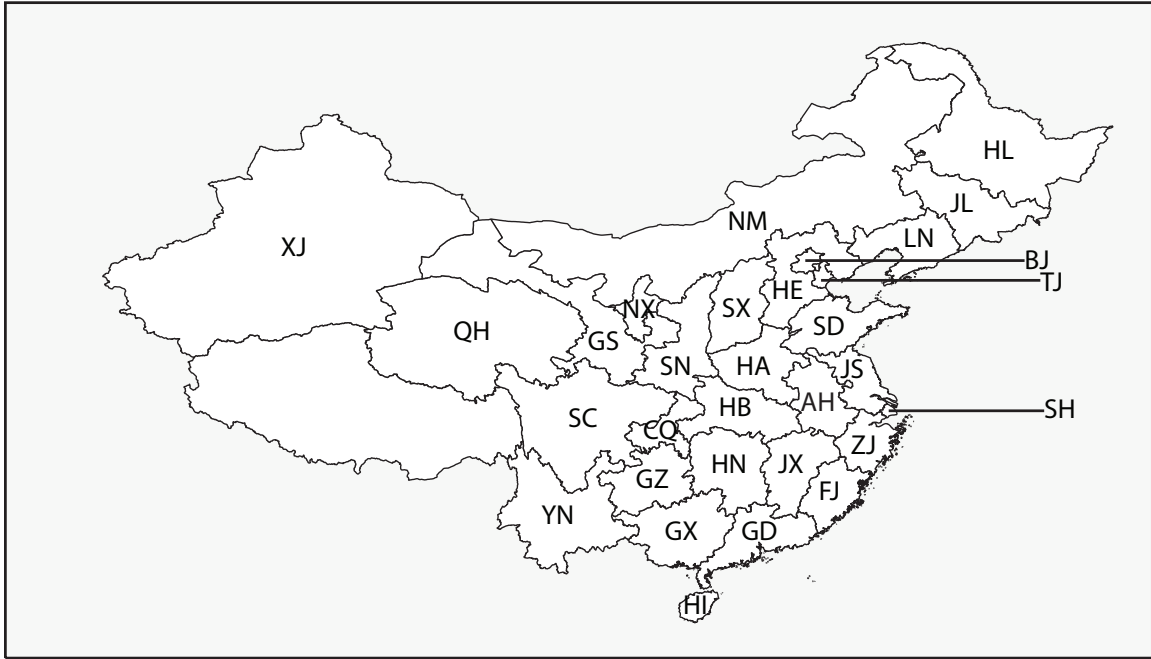


Figure 2-1: Chinese Provinces Evaluated by C-REM

Table 2.2: C-REM Sectors Used to Project Mercury Emissions

| Sector Identifier | Description |
|--------------------------|--|
| COL | Coal mining and processing |
| OMN | Metal minerals mining, non-metal minerals and other mining |
| EIS | Energy intensive industries |
| MAN | Other manufacturing industries |
| ELE | Electricity and heat |
| c | Private consumption |

and second, evaluating atmospheric transport of those emissions and resulting environmental effects.

Projecting Mercury Emissions Inventories

Several researchers have compiled retrospective mercury emissions inventories at various spatial scales for a range of economic sectors. Some inventories focus on a single sector (Li et al., 2017a; Tian et al., 2010), while others focus on a single country. The EPA assembles data on mercury emissions in the United States down to the county level across several sectors in the National Emissions Inventory (US EPA, 2014). Streets et al. (2005), Wu et al. (2016), and Zhang et al. (2015) assembled inventories focused on China at the provincial level for various sectors across the economy.

While single-sector and single-country inventories are useful for understanding trends within a specific nation or economic sector, world-wide retrospective inventories work best for studies that employ a global model. Streets et al. (2017) created an inventory of “all-time anthropogenic [mercury] environmental releases” to land, water, and the atmosphere from 1850 to 2010, evaluated using the global biogeochemical mercury box model from Amos et al. (2013). They provide sector-level detail for 18 different source categories; however, the spatial resolution is fairly coarse as it is organized into 17 world regions. In this study, I use the publicly available EDGARv4 global inventory of speciated atmospheric mercury emissions from various sectors across the world at a spatial resolution of $0.1^\circ \times 0.1^\circ$ compiled by the Joint Research Centre of the European Commission (European Commission, 2014; Muntean et al., 2014). The EDGARv4 inventory includes mercury emissions from 1970 to 2008, calculated using a consistent methodology across decades, and organized into sectors using the same specifications as the IPCC reporting requirements for greenhouse gases (European Commission, 2014; Muntean et al., 2014; IPCC, 1996). Muntean et al. (2014) evaluated the EDGARv4 inventory using a chemical transport model (GEOS-Chem) and found that model simulations performed with the inventory satisfactorily reproduced wet deposition fluxes and total gaseous mercury concentrations. I use the EDGARv4 inventory to analyze mercury co-benefits of climate policy due to its high spatial resolution, sector specification, and successful recreation of global mercury trends with a chemical transport model.

While I project mercury emissions from the EDGAR database myself, some inventories include projections of emissions on the basis of future policy scenarios. Chen et al. (2013) created a county-level inventory for mercury emissions associated with biomass burning for China projected to 2020 using scenario analysis based on institutional data. Pacyna et al. (2010), Pacyna et al. (2016), Streets et al. (2009), and Rafaj et al. (2013) produced global inventories that include projections beyond 2020, utilizing various policy scenarios such as IPCC development scenarios, climate policy, and end-of-pipe control regulations. Pacyna et al. (2010) also utilizes a scenario analysis approach based on expert analyses of future trends and institutional data, creating an inventory with a spatial resolution of $0.5^\circ \times 0.5^\circ$. Pacyna et al. (2016), Streets et al. (2009), and Rafaj et al. (2013) take a modeling-based approach to project emissions in combination with scenario analysis. Pacyna et al. (2016) compiled data on future

energy use from the International Energy Agency, as well as sector-specific economic data at the national level to produce an inventory with spatial resolution of $0.5^\circ \times 0.5^\circ$. They projected economic data to 2035 using national gross domestic product (GDP) per capita data and a regression model. Streets et al. (2009) utilize projections of energy use and fuel mix from the global IMAGE model to scale mercury emissions to 2050 under IPCC economic development scenarios grouped by world regions. Finally, Rafaj et al. (2013) used the Greenhouse Gas and Air Pollution Interactions and Synergies (GAINS) model coupled with the global POLES energy-system model to project global emissions to 2050 with a spatial resolution of $0.5^\circ \times 0.5^\circ$. GAINS uses activity data, uncontrolled fuel and waste emission factors for mercury, and air pollution control device (APCD) technology factors. POLES projects activity data to 2050. Although these inventories comprehensively evaluate future trends in emissions for the whole globe, none of them evaluate specific details of China's economy in their projections, nor are they designed to investigate potential opportunities for co-benefits.

Evaluating Atmospheric Transport and Deposition of Mercury

Studying emissions alone is not enough to understand the full environmental impact of mercury pollution and policy; researchers also evaluate other aspects of mercury's biogeochemical cycle. Researchers use atmospheric transport models to evaluate near-term levels of mercury air concentrations and deposition at various spatial scales to get at short-term impacts of policy scenarios (Pacyna et al. (2016), a global study; Giang & Selin (2016), a US study; Rafaj et al. (2014), a Europe study; Shih & Tseng (2015), a Taiwan study; and Giang et al. (2015), a study on Southeast Asia).

The study performed by Giang et al. (2015) is particularly relevant to this analysis. They evaluate 2050 mercury emissions and total deposition from coal-fired power plants in China and India under end-of-pipe control technology scenarios and IPCC economic development scenarios. The baseline emissions inventory is built using an emissions factor approach with economic activity and mercury coal content data from Streets et al. (2009). The activity factors are representative of the A1B and B1 IPCC development scenarios. A1B represents business-as-usual development, and B1 represents development resulting in decarbonization (and thus lower coal use) in national economies across the world. They generate end-of-pipe control technology scenarios inspired by the Minamata Convention on Mercury based on a literature review and interviews with experts. Giang et al. (2015) evaluate deposition at the national scale in China and India under the various policy scenarios using GEOS-Chem, a global chemical transport model.

Results from the emissions projections performed by Giang et al. (2015) are shown in Figure 2-2. They find that even with no additional controls on end-of-pipe technology in both China and India, emissions are lower in the B1 development scenario case than the A1B case. This indicates that climate policy that leads to decarbonization of the economy could lead to substantial mercury co-benefits in emissions reductions.

There are several limitations to the study performed by Giang et al. (2015). The economic development scenario they use to represent a global decarbonized economy,

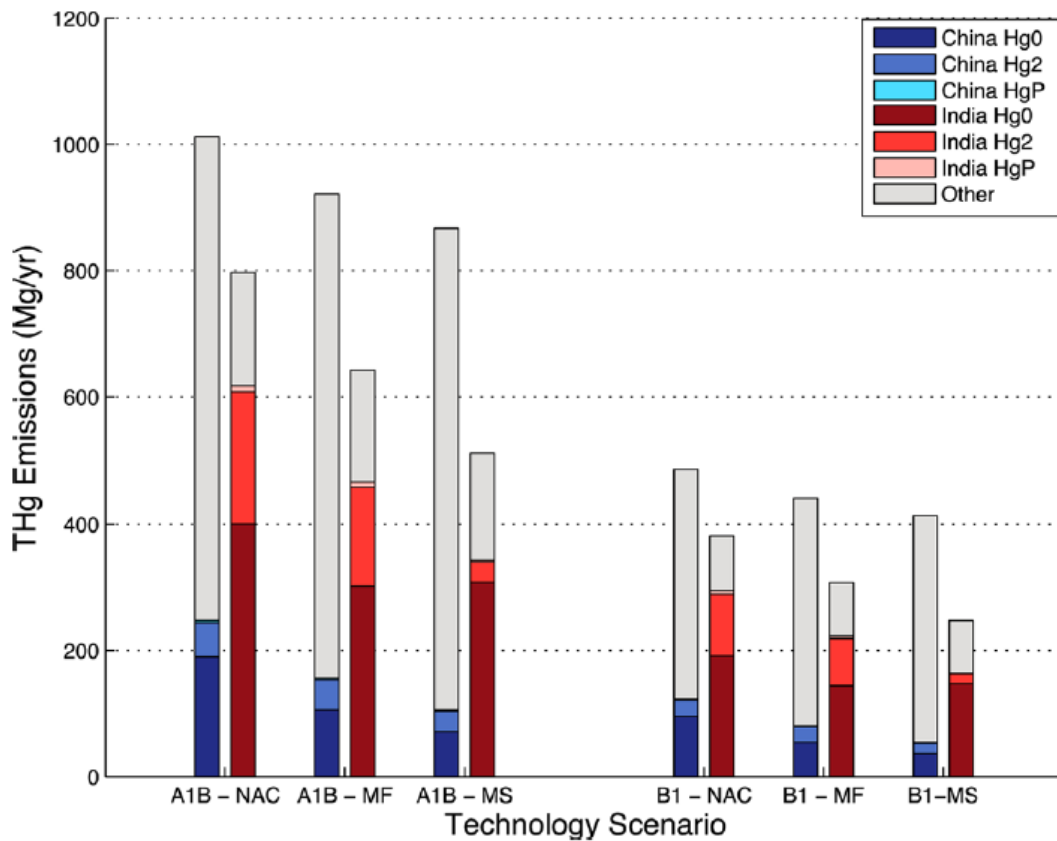


Figure 2-2: 2050 Emissions Projection Results, Giang et al. (2015)
 A1B Represents Business-as-Usual Economic Development, B1 Represents
 Decarbonized Economic Development

B1, comes from the 2000 IPCC Special Report on Emission Scenarios and does not consider implementation of climate policy (van Vuuren & Carter, 2014). Additionally, the scope of policy scenarios and mercury emission sectors is narrow. They evaluate only one climate-related scenario and one sector, power generation emissions.

Mercury Co-Benefits of Climate and Air Pollution Policy

Few researchers have considered mercury co-benefits of air pollution regulation and climate policy from the perspective of both emissions and deposition. Zhao et al. (2015) produced a mercury emissions inventory for China covering several economic sectors, and they project emissions to 2030 under climate policy, end-of-pipe control technology scenarios, and industrial process changes using China national economic data with province-level detail. Zhang et al. (2016b) evaluate the 2030 mercury co-benefit of air pollution policies in China that target particulate matter, NO_x , and SO_x in addition to mercury.

The study performed by Zhang et al. (2016b) is particularly relevant to this analysis. They use an emissions database compiled with probabilistic methods, aiming to reduce uncertainty compared to deterministic emissions inventories (Zhang et al., 2015). They project emissions from coal-fired power plants and coal-fired industrial boilers on the basis of expected coal consumption to 2030 under several of China’s air pollution control regulations that were in place as of 2010, including the Action Plan for Prevention and Control of Air Pollution (“Ten Measures”), the Emission Standard of Air Pollutants for Thermal Power Plants (GB 13223-2011), and the Emission Standard of Air Pollutants for Boilers (GB 13271-2014). The business-as-usual APCD adoption scenario provides an estimate of future APCD adoption across China in 2030 under these existing air pollution control regulations. The accelerated control technology scenario is aligned with China’s commitments under the Minamata Convention.

Notably, Pacyna et al. (2016), Rafaj et al. (2014), and Shih & Tseng (2015) perform studies on the mercury co-benefits of climate policy globally, in Europe, and in Taiwan, respectively by examining short-term deposition resulting from policy perturbations. Pacyna et al. (2016) evaluate two scenarios incorporating climate policy of varying stringency, with one representing existing commitments to address climate change (“New Policy”), and the other representing a world with CO_2 atmospheric concentration capped at 450 ppm (“450 ppm”). They conclude that deposition decreases across the world by 20% to 30 % compared to 2013 levels in the New Policy scenario, with the exception of India, where deposition increases. In the 450 ppm scenario, deposition decreases across the world by 30% to 50% compared to 2013 levels. Rafaj et al. (2014) evaluate one climate policy scenario in which Europe generates as much electricity as possible from renewable sources by 2050, in which deposition is reduced by a maximum of 20 $\text{g}/\text{km}^2/\text{yr}$ compared to a baseline scenario. Unlike Pacyna et al. (2016) and Rafaj et al. (2014), Shih & Tseng (2015) does not use a global chemical transport model. Instead, they approximate deposition reductions using deposition velocities, rainfall levels, emissions projections, and an atmospheric dispersion model under two clean energy scenarios, one focused on natural gas de-

velopment and another focused on renewable energy. They conclude that the clean energy scenarios result in a 8%-27% reduction in deposition by 2030 compared to a baseline scenario.

2.2 Methods

I evaluate 2030 mercury co-benefits of climate policy in China under climate policy in two steps. First, I project 2007 mercury emissions from the EDGARv4 database to 2030 using economic data from the C-REM model scenarios documented by Li et al. (2017b). Second, I use the 2030 mercury emissions in China as input to GEOS-Chem, a global chemical transport model, to evaluate China’s regional-level total deposition in 2030, as well as global deposition impacts.

2.2.1 Base Emissions Inventory: EDGARv4.tox1

I use the 2007 mercury emissions from the publicly available EDGARv4.tox1 database as a baseline (European Commission, 2014; Muntean et al., 2014). Using 2007 mercury emissions provides consistency with the C-REM model, which uses economic and emissions data in China from 2007 (Springmann et al., 2015; Zhang et al., 2013, 2016a). EDGAR provides a global emissions inventory of total mercury, Hg^0 , Hg^{2+} , and HgP grouped by economic sector and resolved to a $0.1^\circ \times 0.1^\circ$ grid. The inventory was verified by Muntean et al. (2014) using GEOS-Chem and measurements where available. The inventory’s economic sectors are classified based on the 1996 IPCC Guidelines for National Greenhouse Gas Inventories (European Commission, 2014; IPCC, 1996). Tables 2.3 and 2.4 provide descriptions of the EDGAR economic sectors.

Mercury emissions from several sub-sectors in the EDGAR database allocated to China are negligible or not available, and are not projected to 2030 for any of the future policy scenarios. Within the Residential and Other Industry Combustion sector, oil refinery emissions are negligible for China (Muntean et al., 2014). Additionally, there are no chlor-alkali industry emissions for China (Muntean et al., 2014). Within the Waste sector, only emissions from municipal solid waste are scaled to 2030. The EDGAR database includes only municipal solid waste incineration and agricultural waste burning in China as part of the Waste sector, and not medical waste incineration (Muntean et al., 2014). Agricultural waste burning emissions in China are negligible (Muntean et al., 2014).

2.2.2 Policy Scenarios

Li et al. (2017b) evaluate four 2030 policy scenarios using C-REM, all of which I use in this analysis: a business-as-usual case (described as “No Policy” in Li et al. (2017b), denoted here as BAU) and three climate policy scenarios of increasing stringency. Li et al. (2017b) prescribe climate policy in the C-REM model essentially as a carbon tax. They constrain the model by a percent reduction in carbon intensity, which

Table 2.3: EDGARv4.tox1 Mercury Inventory Economic Sectors

| Sector Identifier | Description |
|-----------------------------|--|
| cement | Cement production |
| chlor ¹ | Chlor-alkali industry and mercury cell technology |
| comb_power_ind ² | Combustion in power generation, and in industry |
| comb_res_oth | Residential combustion, combustion in oil refineries ¹ , and transformation industry combustion |
| gold_A | Artisanal and small-scale gold mining |
| gold_L | Large-scale gold mining |
| iro | Iron and steel production |
| nfe_oth | Production of zinc, copper, lead, and mercury |
| waste | Medical ³ and municipal solid waste incineration; agricultural waste burning ¹ |

¹Negligible for China

²See Table 2.4 for description of sub-sectors.

³Medical waste incineration in China is not included in the EDGAR database (Muntean et al., 2014).

Table 2.4: EDGARv4.tox1 Power Generation and Industry Combustion Sub-Sectors

| IPCC 1996 Code Identifier¹ | Fuel Combustion Activity Description |
|--|---|
| 1A1a | Public electricity and heat production |
| 1A2a | Iron and steel |
| 1A2b | Non-ferrous metals |
| 1A2c | Chemicals |
| 1A2d | Pulp, paper, and print |
| 1A2e | Food processing, beverages, and tobacco |
| 1A2f | Other |

¹European Commission (2014); IPCC (1996).

Table 2.5: Policy Scenarios for Evaluating Mercury Co-Benefits of Climate Policy in China

| | |
|-----------------------------------|--|
| No Policy (BAU) | Business as usual in 2007 projected to 2030 (Li et al., 2017b) |
| Minamata Policy | Business as usual in 2007 projected to 2030, plus end-of-pipe controls compliant with China's commitments under the Minamata Convention on Mercury applied to combustion in power generation and industry sector (Zhang et al., 2016b) |
| 3% Climate Policy Scenario | Reduces carbon intensity in accordance with China's targets prior to the 2015 Paris Climate Agreement |
| 4% Climate Policy Scenario | Reduces carbon intensity in accordance with China's commitments under its Intended Nationally Determined Contribution for the 2015 Paris Climate Agreement |
| 5% Climate Policy Scenario | Reduces carbon intensity to a global mean level for 2030 |

manifests as a price on CO₂. Higher percent reduction in carbon intensity leads to a higher price on CO₂. As a result, the cost of operating a CO₂-intensive industry increases relative to a business-as-usual scenario (Li et al., 2017b).

The 3% climate policy scenario represents the carbon intensity reduction China would achieve in 2030 based on the country’s commitments prior to the 2015 Paris Climate Agreement. The 4% climate policy scenario constrains carbon intensity in accordance with China’s commitments communicated in its Intended Nationally Determined Contribution to the Paris Agreement. The 5% climate policy scenario aligns China’s carbon intensity with the global mean level in 2030.

In addition to the climate policy scenarios prescribed by Li et al. (2017b), I also evaluate a 2030 Minamata Convention policy scenario that implements end-of-pipe controls only. For this case, I apply air pollution control device (APCD) technology application, mercury capture, and mercury speciation factors from the accelerated control technology scenario developed by Zhang et al. (2016b) to EDGAR emissions from Power Generation and Industry Combustion sector. The accelerated control technology scenario represents one option for a national APCD technology fleet compliant with China’s commitments under the Minamata Convention on Mercury (Zhang et al., 2016b). Only the Power Generation and Industry Combustion sector emissions change in this scenario relative to the BAU case. Emissions from the remaining EDGAR sectors are scaled with the same methodology used for 2030 BAU scenario. Table 2.5 provides a summary of the policy scenarios that I use to evaluate mercury co-benefits of climate policy in China.

2.2.3 Projecting Emissions Without Considering APCDs

Speciated mercury emissions from 2007 for each province and sector listed in Table 2.6 are projected to 2030 ($E_{2030,k,p,s,c}$) by directly applying the corresponding C-REM output data for 2007 and 2030 (with the exception of the artisanal and small-scale gold mining sector).

$$E_{2030,k,p,s,c} = E_{2007,k,p,s} \frac{C_{2030,p,s,c}}{C_{2007,p,s,c}}$$

Here, k represents mercury species, p represents the provinces, s represents the EDGAR sector, c represents the policy scenario, $E_{2007,k,p,s}$ is the total EDGAR emissions from EDGAR sector s , and C_{2030} and C_{2007} are C-REM outputs from the applicable sector, year, and policy scenario.

The EDGAR sectors are matched with C-REM output data and economic sectors, as listed in Table 2.6. Emissions from the production processes for cement, iron and steel, non-ferrous metals, and large-scale gold mining are the result of mercury content in the raw materials of these final products, or in commercial products in the case of the waste sector (UNEP, 2013b). As such, the cement, coal transformation industry combustion (a portion of the Residential and Other Industry Combustion sector in EDGAR), large-scale gold mining, iron and steel, and non-ferrous metals smelting sectors are scaled by economic output from the corresponding C-REM sector discussed below. I make the assumption that municipal solid waste is dependent on

Table 2.6: EDGAR Sectors Projected Without Considering APCDs and Corresponding C-REM Sectors and Outputs for Scaling to 2030

| EDGAR Sector | C-REM Scaling Sector | C-REM Output |
|---------------------|-----------------------------|----------------------------------|
| cement | EIS | Economic Output |
| comb_res_oth | c COL | CO2 Emissions Economic Output |
| gold_A | Not Scaled | Not scaled |
| gold_L | OMN | Economic Output |
| iro | EIS | Economic Output |
| nfe_oth | EIS | Economic Output |
| waste | c | Economic Output |

household income, so the waste sector is also scaled by economic output from C-REM private consumption sector (note that mercury use in commercial products will be phased down under the Minamata Convention, see discussion below). Finally, I scale emissions from residential combustion with CO₂ emissions from C-REM.

The C-REM energy intensive sector (EIS) includes iron and steel, non-ferrous metals and non-metallic materials processing, and the chemical industry. As such, the EDGAR cement, iron and steel, and non-ferrous metals sectors are scaled with C-REM EIS. I scale the EDGAR coal transformation industry emissions with the C-REM coal (COL) sector and the EDGAR large-scale gold mining emissions with the C-REM mining (OMN) sector (Springmann et al., 2015; Zhang et al., 2013, 2016a). Finally, since both residential combustion and waste are linked with households, I scale emissions from these EDGAR sectors with the C-REM private consumption sector.

For the purposes of this study, I do not consider changes in existing emission control measures. This is a realistic approach because current regulations in place likely will not change the adoption of APCDs that affect mercury emissions in these sectors significantly. For the cement, iron and steel, non-ferrous metals smelting, large-scale gold mining, and residential and other industry combustion sectors, this approach is supported by Wu et al. (2016) and Zhao et al. (2015). Wu et al. (2016) investigate retrospective temporal trends in China from 1978-2014 and draw conclusions about the potential for additional abatement from several mercury-relevant sectors. They find that significant reductions in mercury emissions from cement production are possible; however, there are currently no policies in place to incentivize adoption. Additionally, they conclude that APCDs have already been widely adopted to control emissions from non-ferrous metals smelting processes (pointing to the example of zinc) and that there is little room for improving mercury emissions abatement in this sector.

Zhao et al. (2015) project emissions control trends to 2030 for the sectors I consider in this section as well as some other mercury-relevant sectors. Their conclusion on

non-ferrous metals smelting, large-scale gold mining, and iron and steel production is aligned with the conclusions from Wu et al. (2016). However, I note that Zhao et al. (2015) project that all cement kilns will adopt precalciner technology with fabric filters by 2030, which leads to a reduction in cement sector mercury emissions of about 30 percent compared to their 2015 case. Wu et al. (2016) note that dry-process precalciner kilns reuse the mercury-containing dust captured by fabric filters, leading to a null benefit in mercury emissions reductions. They also note that dust shuttling technology could be used to capture mercury from the fabric filter dust, but there are currently no regulations in place to incentivize such a technology. Zhao et al. (2015) does not provide information on dust re-use in precalciner kilns or dust shuttling technology. Therefore, I follow the conclusions of Wu et al. (2016) for the cement sector.

Zhao et al. (2015) and Wu et al. (2016) do not consider APCDs for the residential sector since few control options exist for residential combustors.

Within the waste sector, only municipal solid waste incineration EDGAR emissions from China are relevant for projection to 2030, as discussed above. Mercury has historically been used in commercial products such as paint, lightbulbs, batteries, electrical switches and relays, thermostats, barometers, manometers, thermometers, blood pressure meters, vaccines and medicines, soaps, cosmetics, dyes, pesticides, fertilizers, and fireworks (Horowitz et al., 2014). Mercury-added products are set to be phased-out by 2020 under the Minamata Convention (UNEP, 2013a). Reductions in emissions from this sector will likely be driven by the decreased use of mercury in commercial and consumer products, so APCDs were not considered for this sector (Wu et al., 2016; Horowitz et al., 2014). Additionally, I do not consider a gradual reduction in emissions from the Waste sector. Mercury-added products will be permitted for 13 years following the base year of 2007, and many of these products have a considerably long useful lifetime.

For the artisanal and small-scale gold mining sector, I do not scale 2007 emissions to 2030, but they are included with the projected emissions for the chemical transport and deposition analysis since they comprise a large portion of emissions from China within the EDGAR database (see Figure 2-3). I note that small-scale gold mining is technically illegal in China, and the country does not provide official statistics on economic activity or emissions from this sector (Wu et al., 2016; Telmer & Veiga, 2009). As a result, emissions from the EDGAR artisanal and small scale gold mining sector are compiled based on the market demand for gold (Muntean et al., 2014; Telmer & Veiga, 2009). Muntean et al. (2014) suggest that emissions from artisanal and small scale gold mining could also be driven by poverty levels in a given country. In any case, climate policy is not likely to have direct impacts on the market for gold or poverty in China.

Table 2.7: EDGAR Sectors Projected With Consideration of APCDs and Corresponding C-REM Sectors and Outputs for Scaling to 2030

| EDGAR Sector | C-REM Scaling Sector | C-REM Output |
|---|----------------------|----------------------|
| comb_power_ind 1A1a: Electricity and heat | ELE | Energy Use from Coal |
| 1A2a: Iron and steel 1A2b: Non-ferrous metals 1A2c: Chemicals | EIS | |
| 1A2d: Pulp, paper, print 1A2e: Food, beverages, tobacco 1A2f: Other | MAN | |

2.2.4 Projecting Emissions to Account for Future Changes in APCDs: Power Generation and Industry Combustion

Table 2.7 shows the Power Generation and Industry Combustion sector disaggregated into its sub-sectors and matched with C-REM sectors and outputs. All sub-sectors are scaled using C-REM output on energy use from coal. This is aligned with the emissions factor methodology utilized by Streets et al. (2009) and Giang et al. (2015). The EDGAR sub-sectors are matched to applicable C-REM sectors. In C-REM, the energy-intensive sector (EIS) includes iron and steel, non-ferrous metals and non-metallic materials processing, and the chemical industry (Li et al., 2017b). The remaining Power Generation and Industry Combustion sub-sectors are comparatively less energy-intensive, including pulp, paper, print; food, beverage and tobacco; and other mercury emissions and are accordingly matched to the manufacturing C-REM sector (Springmann et al., 2015; Zhang et al., 2013, 2016a).

I consider changes to APCDs applied to coal fired power plants and coal fired industrial boilers that are currently planned under existing energy and environmental regulations for the 2030 climate policy scenarios. Combustion from power generation and industry in the EDGAR database accounted for approximately 30 percent of China’s mercury emissions in 2007 (as shown in Figure 2-3). Current Chinese regulations such as the Action Plan for Prevention and Control of Air Pollution (the “Ten Measures”), Emission Standard of Air Pollutants for Thermal Power Plants (GB13223-2011), and the Emission Standard of Air Pollutants for Boilers (GB13271-2014) will likely translate to wider adoption of APCDs to coal fired power plants and coal fired industrial boilers into the future according to Zhang et al. (2016b). Additionally, emissions from this sector are likely to be heavily influenced by climate policy.

I also rely on APCD technology information to project Power Generation and Industry Combustion emissions under the Minamata Convention policy scenario that considers end-of-pipe controls only.

I incorporate APCD adoption into emissions projections for the climate policy

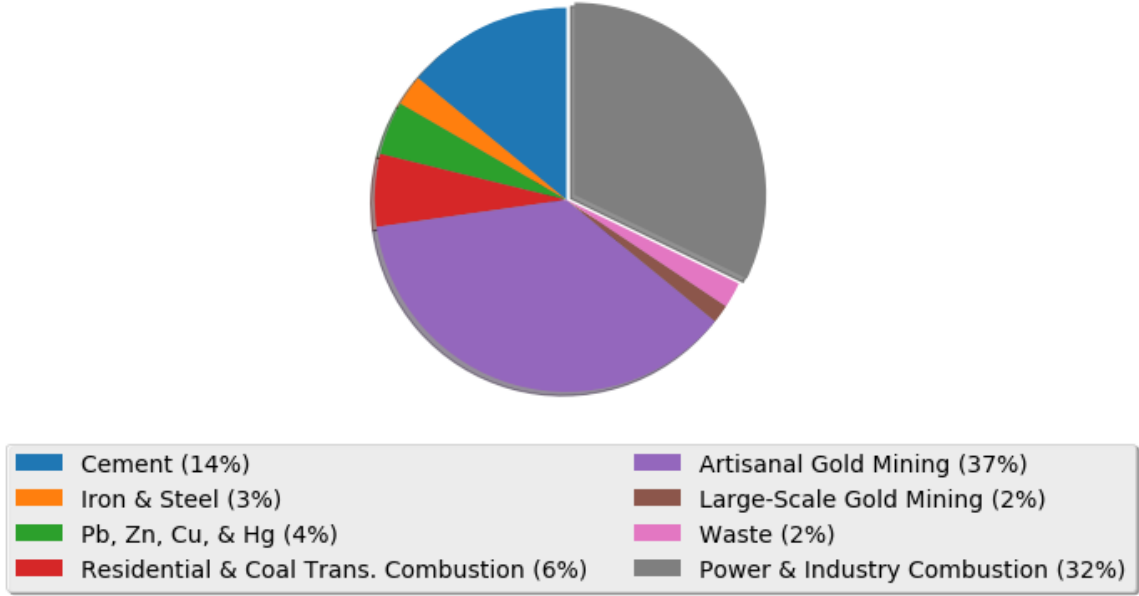


Figure 2-3: 2007 EDGAR Emissions, China (Muntean et al., 2014)

and Minamata Convention cases by applying the business-as-usual and accelerated control technology scenario, respectively, from Zhang et al. (2016b). I perform the emission projection in two steps for each of the 2030 policy scenarios. First, I determine the total uncontrolled mercury emissions in 2030 in a given province and sub-sector ($E_{uc,2030,p,s,c}$) by applying the 2010 national APCD technology information from Zhang et al. (2016b) and summing across the full technology scenario.

$$E_{uc,2030,p,s,c} = \sum_i \frac{f_{app,i}}{(1 - f_{cap,i})} E_{c,2007,p,s} \frac{C_{2030,p,s,c}}{C_{2007,p,s,c}}$$

Here, i represents the APCD configurations for 2010 from Zhang et al. (2016b), $f_{app,i}$ is the application fraction, and $f_{cap,i}$ is the capture efficiency, and $E_{c,2007,p,s}$ is the total EDGAR emissions from the Power Generation and Industry Combustion sub-sectors, grouped according to Table 2.7. Values for f_{app} and f_{cap} are provided in Table 2.8.

Second, I apply 2030 APCD technology information to obtain the 2030 controlled, speciated mercury emissions (Hg^0 , Hg^{2+} , HgP , denoted as k in the equation below) under the climate policy and Minamata Convention scenarios in each province and sub-sector.

$$E_{c,2030,k,p,s,c} = \sum_j f_{spec,j,k} f_{app,j} (1 - f_{cap,j}) E_{uc,2030,p,s,c}$$

Here, $E_{c,2030}$ is controlled mercury emissions, k represents mercury species, j represents the business-as-usual APCD configurations for 2030 from Zhang et al. (2016b), and f_{spec} is the speciation factor. Values for $f_{app,j}$ and $f_{cap,j}$ are provided in Tables 2.9 and 2.11, and values for $f_{spec,j,k}$ are provided in Tables 2.10 and 2.12.

2.2.5 Transport and Deposition

I use a chemical transport model, GEOS-Chem Version 11-01, to evaluate transport and deposition of mercury emissions under the 2030 climate policy scenarios. GEOS-Chem is a global, 3-D chemical transport model that uses meteorology from the Goddard Earth Observing System (GEOS) of the NASA Global Modeling and Assimilation Office (Bey et al., 2001). It has been used to evaluate mercury transport and deposition in several studies (Corbitt et al., 2011; Horowitz et al., 2014; Wang et al., 2014; Giang et al., 2015; Giang & Selin, 2016). GEOS-Chem models all three species of mercury. In the model, Hg^0 is emitted by both natural and anthropogenic sources, while Hg^{2+} and HgP are emitted only by anthropogenic sources (Giang et al., 2015). I input the full set of global mercury emissions as the sum of the 2030 China emissions, 2007 artisanal and small scale gold mining emissions from China, and the 2007 EDGARv4.tox1 emissions for the rest of the world using the Harvard-NASA Emissions Component (HEMCO) feature of GEOS-Chem (Keller et al., 2014).

The chemical transport modeling methodology described here is based on Giang et al. (2015). I use present-day meteorology in order to isolate the effect of inter-annual climate variability on mercury transport and deposition from the GEOS-5 meteorology field. I run the model for three years (2004-2006) to establish initial conditions. I use the standard mercury simulation settings for oxidation, reduction, natural emissions, soil mercury distribution, biomass burning, and ocean dynamics. Details on chemistry and biogeochemical cycling mechanisms are documented in Giang et al. (2015) and summarized here. The model reads in the sum of Hg^{2+} plus HgP emissions and determines the equilibrium speciation based on gas-particle partitioning coefficients evaluated by Amos et al. (2012). Hg^0 is oxidized to Hg^{2+} by bromine, and Hg^{2+} is reduced back to Hg^0 in cloud water following the analysis conducted by Holmes et al. (2010). Mercury cycles with land based on the terrestrial model developed by Selin et al. (2008), and mercury cycles with the ocean based on the 2-D slab model developed by Soerensen et al. (2010). Dry deposition is calculated using a resistance-in-series model that considers aerodynamic resistance, boundary resistance, and tree canopy surface resistance (Bey et al., 2001). Wet deposition is calculated considering rainout, washout, and scavenging in convective updrafts (Liu et al., 2001).

Total deposition (wet plus dry) results are presented as a three-year average (2007-2009) at a resolution of $4^\circ \times 5^\circ$, overlaid with China's provincial boundaries in order to evaluate the effect of climate policy at the regional level in China. Total deposition results from the climate policy and Minamata Convention scenarios (see Table 2.5) are subtracted from the 2030 BAU case in order to isolate the impact of legacy re-emissions from land and the ocean.

Table 2.8: 2010 APCD Application and Mercury Capture Factors

| EDGAR comb_power_ind Sub-Sector | APCD Configuration | f_{app}^1 | f_{cap}^1 |
|---------------------------------|--------------------|-------------|-------------|
| 1A1a: Electricity and heat | SCR+ESP+WFGD | 0.11 | 0.69 |
| | SCR+FF+WFGD | 0.01 | 0.93 |
| | FF+WFGD | 0.06 | 0.86 |
| | ESP+WFGD | 0.74 | 0.62 |
| | ESP | 0.07 | 0.29 |
| | FF | 0.01 | 0.67 |
| 1A2a: Iron and steel | FF+WFGD | 0.12 | 0.86 |
| 1A2b: Non-ferrous metals | WS | 0.48 | 0.23 |
| 1A2c: Chemical | IMS | 0.40 | 0.38 |
| 1A2d: Pulp, paper, print | | | |
| 1A2e: Food, beverages, tobacco | | | |
| 1A2f: Other | | | |

SCR=selective catalytic reduction, ESP=electrostatic precipitator, WFGD=wet flue gas desulfurization, FF=fabric filter, WS=wet scrubber, IMS=integrated marble scrubber

¹ Zhang et al. (2016b)

Table 2.9: 2030 Business-as-Usual APCD Application and Mercury Capture Factors

| EDGAR comb_power_ind Sub-Sector | APCD Configuration | f_{app}^1 | f_{cap}^1 |
|--|---------------------------|-------------|-------------|
| 1A1a: Electricity and heat | SCR+ESP+WFGD | 0.50 | 0.69 |
| | SCR+FF+WFGD | 0.10 | 0.93 |
| | FF+WFGD | 0.10 | 0.86 |
| | ESP+WFGD | 0.25 | 0.62 |
| | ESP | 0.05 | 0.29 |
| 1A2a: Iron and steel | SCR+FF+WFGD | 0.10 | 0.93 |
| 1A2b: Non-ferrous metals | FF+WFGD | 0.25 | 0.86 |
| 1A2c: Chemical | WS | 0.20 | 0.23 |
| 1A2d: Pulp, paper, print | IMS | 0.45 | 0.38 |
| 1A2e: Food, beverages, tobacco | | | |
| 1A2f: Other | | | |

¹ Zhang et al. (2016b)

Table 2.10: 2030 Business-as-Usual APCD Speciation Factors

| EDGAR Sub-Sector (comb_power_ind) | APCD Configuration | f_{spec,Hg^0}^1 | $f_{spec,Hg^{2+}}^1$ | $f_{spec,HgP}^1$ |
|--|-------------------------------|-------------------|----------------------|------------------|
| 1A1a: Electricity and heat | SCR+ESP+WFGD | 0.739 | 0.259 | 0.002 |
| | SCR+FF+WFGD ² | 0.68 | 0.32 | 0 |
| | FF+WFGD | 0.78 | 0.21 | 0.01 |
| | ESP+WFGD | 0.837 | 0.157 | 0.006 |
| | ESP | 0.58 | 0.41 | 0.01 |
| 1A2a: Iron and steel | SCR+FF+WFGD ³ | 0.68 | 0.32 | 0 |
| 1A2b: Non-ferrous metals | FF+WFGD ³ | 0.78 | 0.21 | 0.01 |
| 1A2c: Chemical | WS | 0.65 | 0.33 | 0.02 |
| 1A2d: Pulp, paper, print | IMS ⁴ | 0.65 | 0.33 | 0.02 |
| 1A2e: Food, beverages, tobacco | | | | |
| 1A2f: Other | | | | |

¹ Zhang et al. (2016b), unless otherwise noted

² Giang et al. (2015)

³ Assumed same as coal-fired power plants

⁴ Assumed same as WS

Table 2.11: 2030 Minamata Convention APCD Application and Mercury Capture Factors

| EDGAR comb_power_ind Sub-Sector | APCD Configuration | f_{app}^1 | f_{cap}^1 |
|---------------------------------|--------------------|-------------|-------------------|
| 1A1a: Electricity and heat | SCR+ESP+WFGD | 0.09 | 0.69 |
| | SCR+FF+WFGD | 0.36 | 0.93 |
| | SNCR+FF+WFGD | 0.05 | 0.84 ² |
| | SMC+SCR+ESP+WFGD | 0.50 | 0.90 ³ |
| 1A2a: Iron and steel | SCR+FF+WFGD | 0.60 | 0.93 |
| 1A2b: Non-ferrous metals | FF+WFGD | 0.20 | 0.86 |
| 1A2c: Chemical | IMS | 0.20 | 0.38 |
| 1A2d: Pulp, paper, print | | | |
| 1A2e: Food, beverages, tobacco | | | |
| 1A2f: Other | | | |

SNCR = selective non-catalytic reduction, SMC = mercury-specific technology

¹ Zhang et al. (2016b)

² Assume same capture factor as SNCR+FF on a coal-fired power plant.

³ Adjusted so that average mercury removal efficiency from coal-fired power plants in 2030 is 90% in accordance with the accelerated control technology scenario from Zhang et al. (2016b)

Table 2.12: 2030 Minamata Convention APCD Speciation Factors

| EDGAR Sub-Sector (comb_power_ind) | APCD Configuration | f_{spec,Hg^0}^1 | $f_{spec,Hg^{2+}}^1$ | $f_{spec,HgP}^1$ |
|--------------------------------------|-------------------------------|-------------------|----------------------|------------------|
| 1A1a: Electricity and heat | SCR+ESP+WFGD | 0.739 | 0.259 | 0.002 |
| | SCR+FF+WFGD ² | 0.68 | 0.32 | 0 |
| | SNCR+FF+WFGD ³ | 0.78 | 0.21 | 0.01 |
| | SMC+SCR+ESP+WFGD ⁴ | 0.837 | 0.157 | 0.006 |
| 1A2a: Iron and steel | SCR+FF+WFGD ⁵ | 0.68 | 0.32 | 0 |
| 1A2b: Non-ferrous metals | FF+WFGD ⁵ | 0.78 | 0.21 | 0.01 |
| 1A2c: Chemical | IMS ⁶ | 0.65 | 0.33 | 0.02 |
| 1A2d: Pulp, paper, print | | | | |
| 1A2e: Food, beverages, tobacco | | | | |
| 1A2f: Other | | | | |

¹ Zhang et al. (2016b), unless otherwise noted

² Giang et al. (2015)

³ Assumed same as SCR+FF+WFGD

⁴ Assumed same as SCR+ESP+WFGD

⁵ Assumed same as coal-fired power plants

⁶ Assumed same as WS

2.3 Results and Discussion

In this section, I present results and discussion on the emissions projection and chemical transport modeling analyses at the international level, as well as the national and regional level in China.

2.3.1 Emissions Projections to 2030

Mercury emissions in China increase substantially between 2007 and 2030 under the policy scenarios. All three climate policy scenarios exhibit reduced total mercury emissions ($\text{Hg}^0 + \text{Hg}^{2+} + \text{HgP}$) compared to the BAU case when aggregated to the national level. Increasing climate policy stringency also increases the magnitude of emissions reductions. Notably, the 5% carbon intensity reduction scenario results in a 15% decrease in mercury emissions compared to the BAU case, and the Minamata Convention scenario results in a 17% decrease. Figure 2-4 provides total mercury emissions in China for each policy scenario.

The relative contribution from each economic sector to the national-level emissions reduction varies by policy scenario. As discussed above, only the Power Generation and Industry Combustion sector contributes to the emissions reduction in the Minamata Convention case by design. Power Generation and Industry Combustion emissions reductions contribute only 4% to the overall emissions reductions in the 3% climate policy scenario, whereas this sector contributes approximately 61% of the emissions reductions in both the 4% and 5% climate policy scenarios. In the 3% climate policy scenario, Residential and Coal Transformation Combustion contributes the greatest share of emissions reductions at approximately 42%. Figure 2-5 shows the relative contribution of each sector to the national emissions reductions in each climate policy scenario.

At the regional level, the coastal, central, and southern provinces have the highest total mercury emissions in 2030, and the spatial distribution patterns of Hg^0 and $\text{Hg}^{2+} + \text{HgP}$ are similar, as shown in Figures 2-6 and 2-7 for the BAU case. The distribution of Hg^0 relative to $\text{Hg}^{2+} + \text{HgP}$ emissions by province does not change much across policy scenarios. Sichuan province-level emissions represent the greatest share of total emissions in China at around 7%-8% for each 2030 policy scenario. The contribution of each economic sector varies widely by province, as shown in Figure 2-8 for the BAU case.

The highest magnitude reductions in emissions compared to the BAU case also occur in the coastal, central, and southern provinces, and this holds true across the climate policy and Minamata Convention scenarios. Figure 2-9 shows absolute total mercury emissions for the BAU case, as well as absolute emissions reductions compared to the BAU case for each policy scenario. However, the relative contribution from each province to the national change in mercury emissions compared to the BAU case varies across the climate policy and Minamata Convention scenarios, as shown in Figure 2-10.

The relative contribution to the change in emissions by province varies widely across China in the 3% climate policy scenario, with some provinces exhibiting an

increase in emissions compared to the BAU case and others exhibiting a decrease. However, note that the change in national emissions between the 3% climate policy scenario and BAU case is small. In the 4% climate policy scenario, nearly all provinces exhibit a reduction in emissions, up to a maximum of about 14% in Shanxi. In comparison, several provinces experience a slight increase in emissions in the 5% climate policy scenario, and the highest level of emissions reductions (15%) shifts to Hubei. All provinces exhibit a reduction in emissions in the Minamata Convention scenario, with Shanxi once again exhibiting the highest percent reduction (9%).

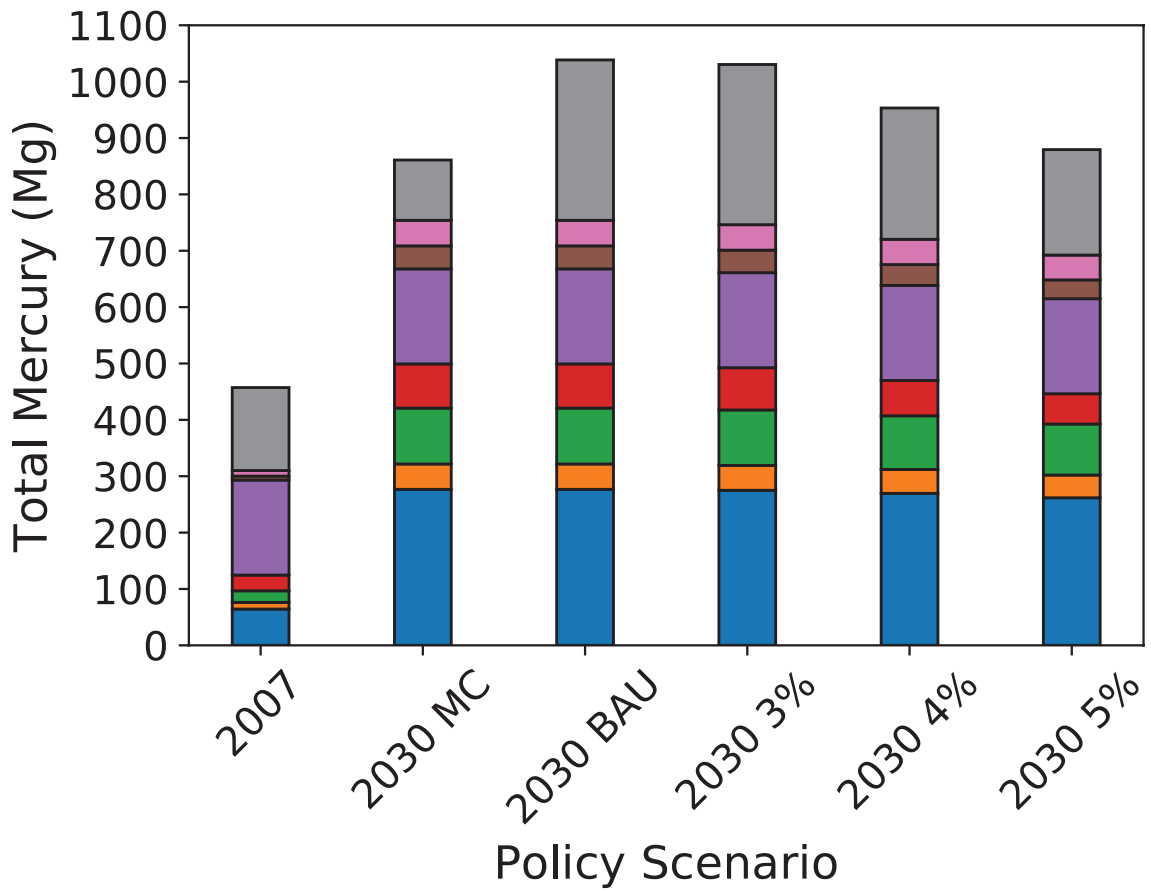


Figure 2-4: Total Mercury Emissions in China, 2030 Policy Scenarios

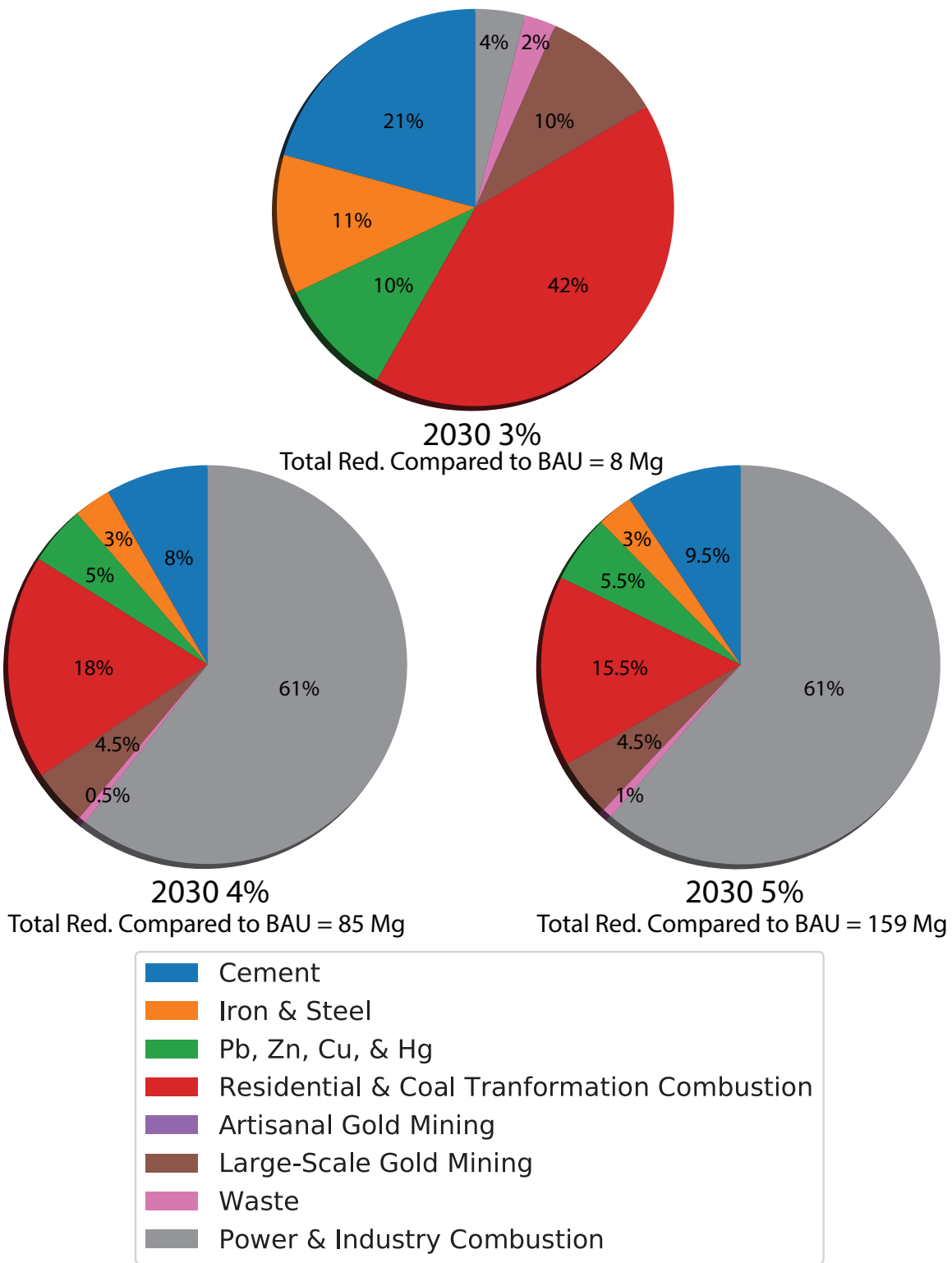


Figure 2-5: Relative Contribution by Sector to National Emission Reductions Compared to 2030 BAU Case

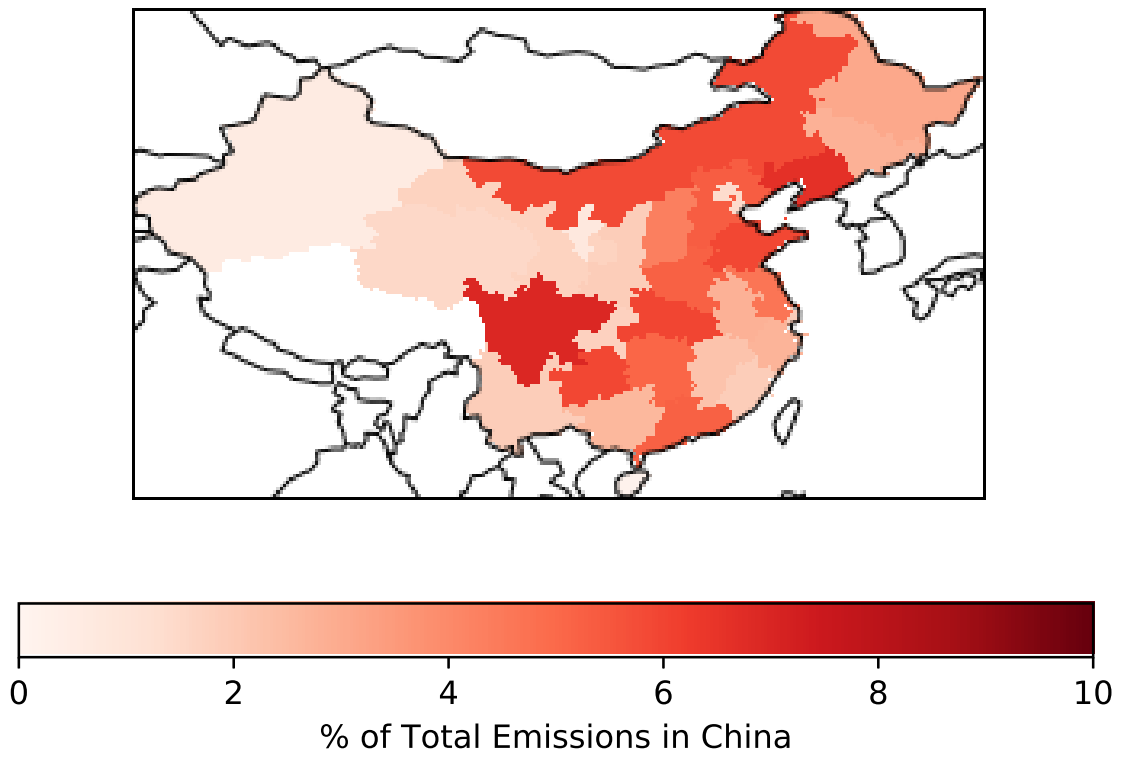
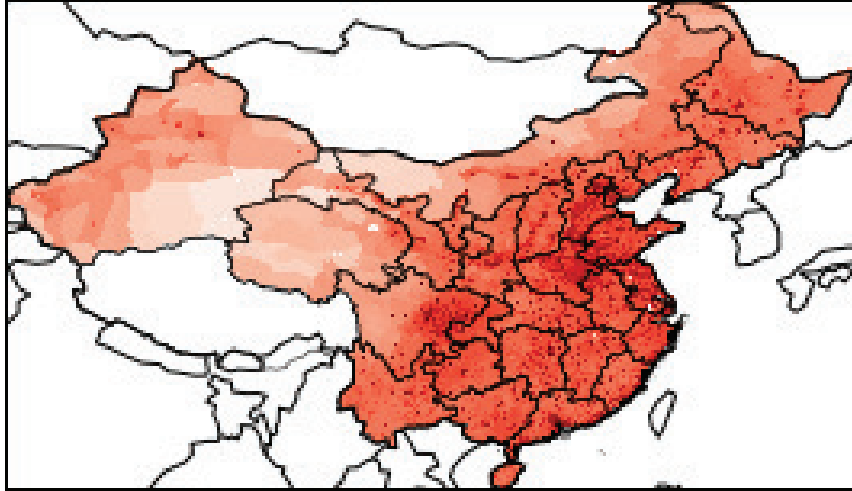


Figure 2-6: Distribution of Total Emissions by Province, 2030 BAU Scenario

2030 BAU Hg(0)



2030 BAU Hg(2) + HgP

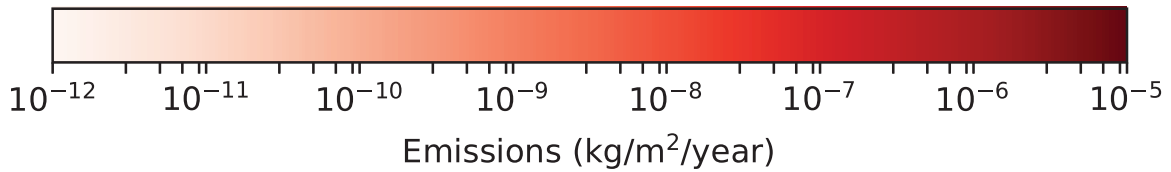
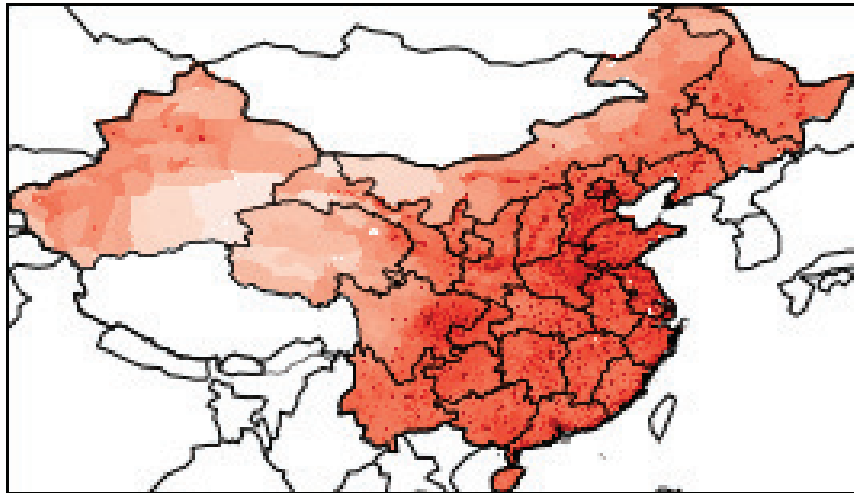


Figure 2-7: Speciated Emissions, 2030 BAU Scenario

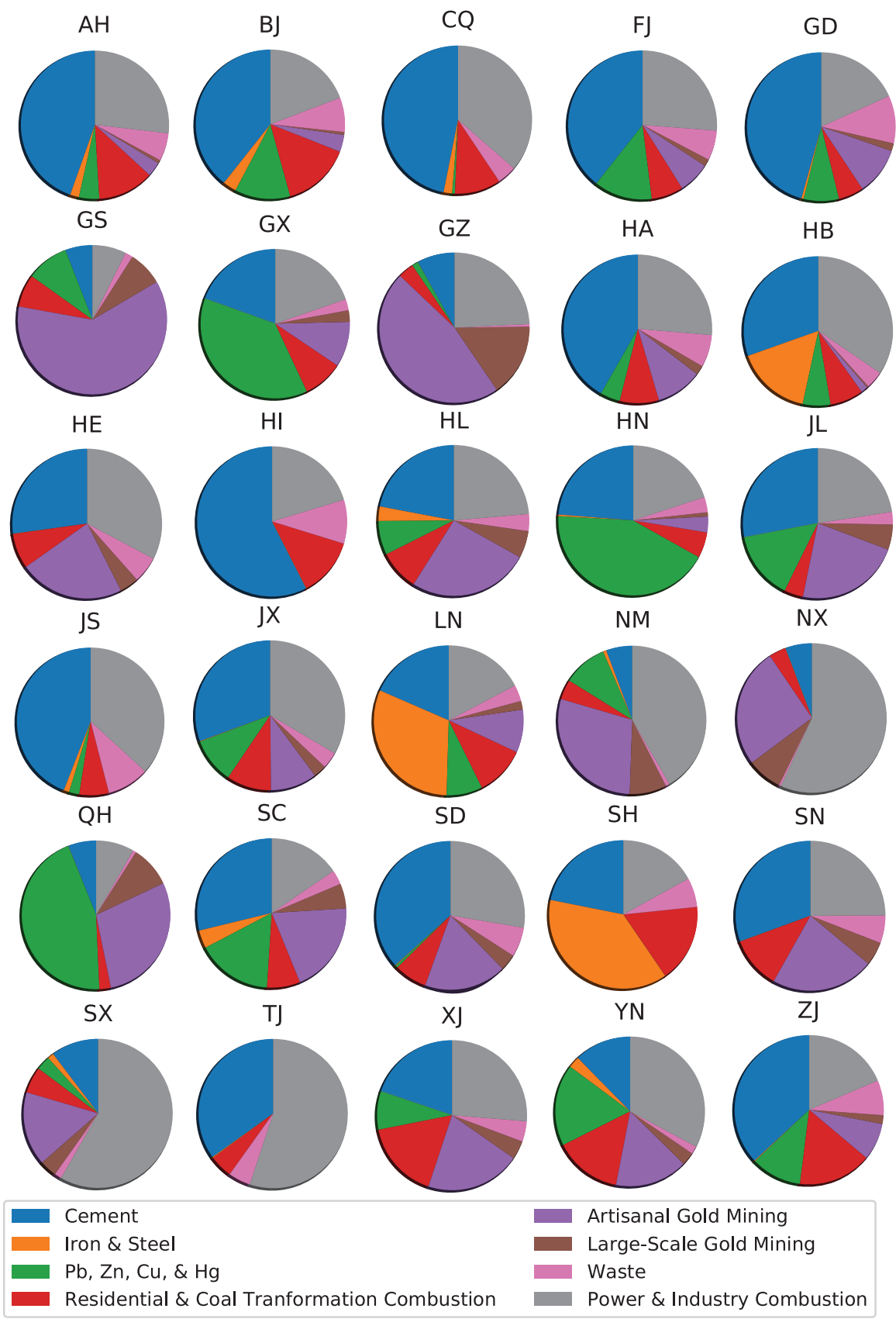


Figure 2-8: Sector Emissions by Province, 2030 BAU Scenario

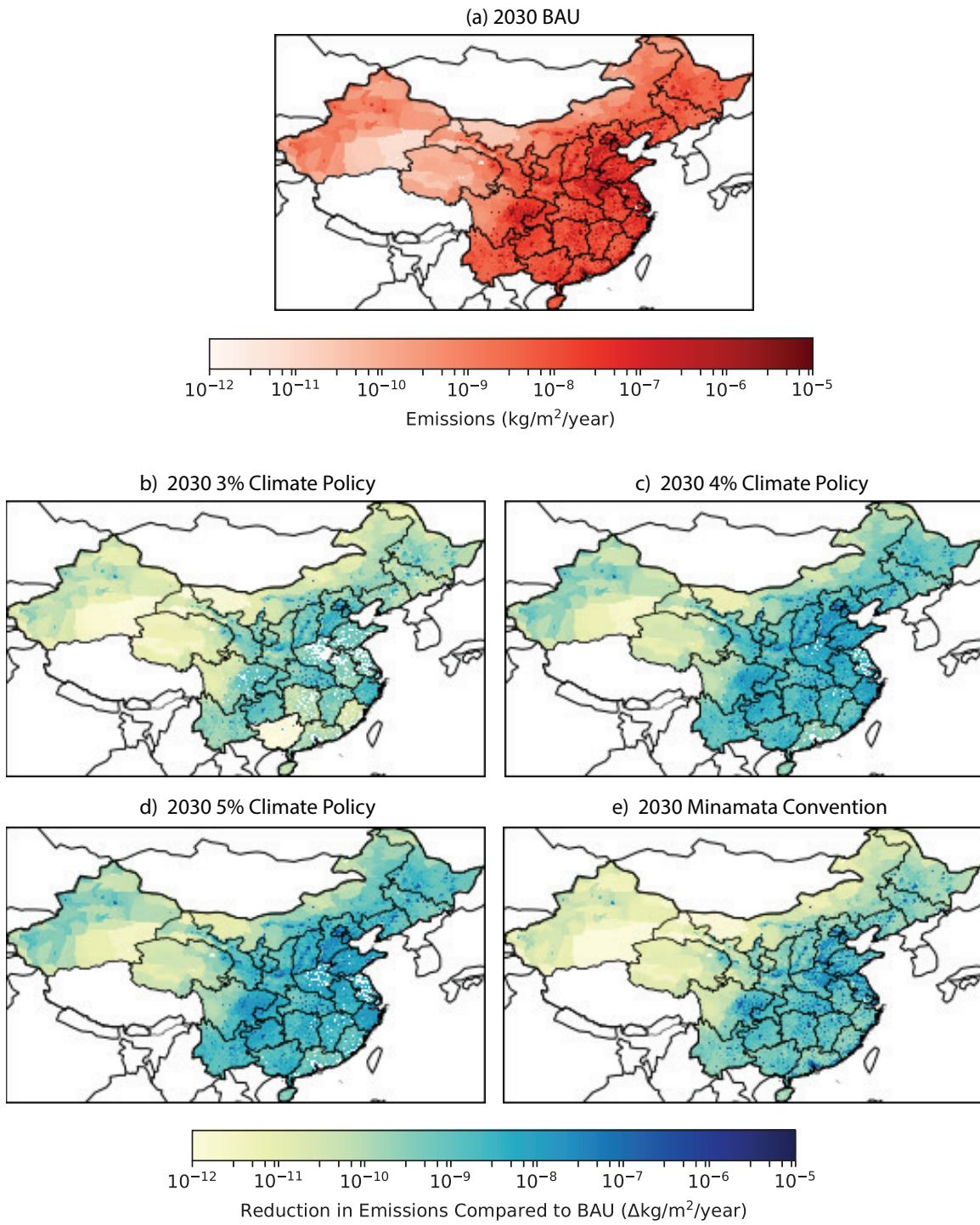


Figure 2-9: Distribution of Total Mercury Emissions in China
 (a) Absolute Emissions, 2030 BAU Case; (b)-(e) Reduction in Emissions Compared to BAU Case

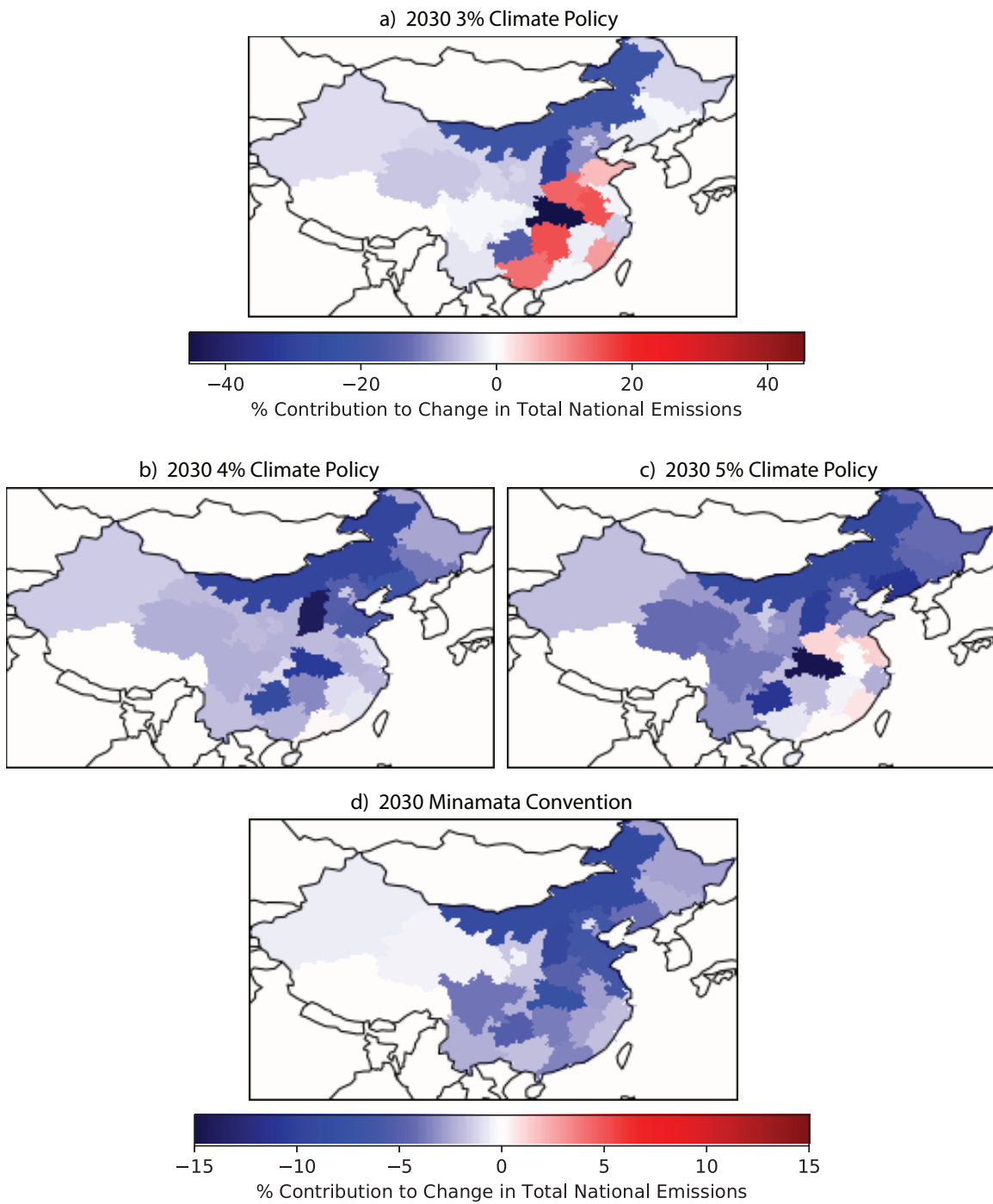


Figure 2-10: Relative Contribution of Emissions Reductions by Province Compared to the 2030 BAU Scenario

2.3.2 Total Deposition in 2030

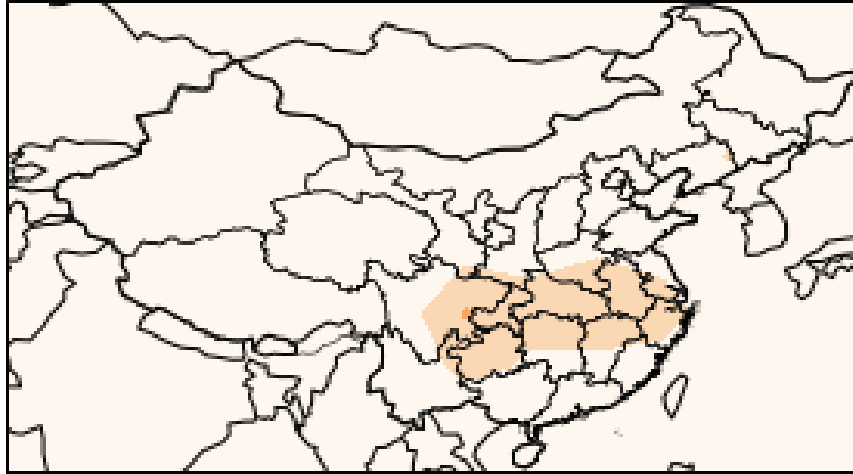
The highest absolute levels of total deposition in 2030 occur in coastal, central, and southern provinces for all policy scenarios. The relative contribution of wet and dry deposition to total deposition does not vary across the policy scenarios. Figure 2-11 shows wet and dry deposition for the 2030 BAU case.

The percent difference in total deposition by province compared to the BAU case varies across the policy scenarios, as shown in Figure 2-12. The 3% climate policy scenario exhibits small changes in total deposition relative to the BAU case, with deposition increasing in some of the southern provinces. All provinces experience a decrease in total deposition in the 4% climate policy, 5% climate policy, and Minamata Convention scenarios compared to the BAU case. The highest levels of reduction in total deposition occur in the coastal, central, and southern provinces, with maximum reductions centered over Shanxi. The 5% climate policy and Minamata Convention scenarios exhibit the highest reductions in total deposition compared to the BAU case of all the policy scenarios at about 25%.

Deposition in some areas outside of China decreases in the climate policy and Minamata Convention scenarios. Figure 2-13 shows absolute total deposition for the BAU case across the world, and Figure 2-14 shows percent difference in global deposition compared to the BAU case for the 4% climate policy scenario, 5% climate policy scenario, and Minamata Convention scenario (the 3% climate policy case is not pictured here since it shows very small changes in deposition outside of China). The 4% climate policy scenario shows small reductions in deposition (less than 3%) in the northern Pacific Ocean as far east as the West Coast of the United States. The 5% climate policy scenario shows deposition reductions between 3% and 5% in the same area, in addition to deposition reduction benefits of approximately 1% to 3% in the northern hemisphere and most of the southern hemisphere. Finally, the Minamata Convention case shows deposition reductions of approximately 3% to 5% in the northern hemisphere, and deposition reductions of approximately 1% to 3% in the southern hemisphere down to approximately the Antarctic circle.

Table 2.13 summarizes total emissions and deposition in Mg for all policy scenarios, comparing China and the rest of the world. Emissions include anthropogenic emissions, geogenic emissions, soil emissions, biomass burning emissions, land re-emissions, snow emissions, and ocean up flux. Total deposition includes wet and dry deposition as well as Hg^{2+} deposition to sea salt. The table shows absolute mercury emissions and deposition for the BAU case and each of the other policy scenarios, along with the change in emissions and deposition between the BAU case and policy scenarios. This data is provided globally, for China, and for the rest of the world (ROW). Additionally, for each policy scenario, the table provides the percent contribution to the change in total deposition compared to the BAU case for China and the rest of the world. About 30%-40% of the global reduction in total deposition compared to the BAU case occurs within China, and the remaining 60%-70% occurs in the rest of the world in all policy scenarios, although the reductions are spatially distributed across the globe, as shown in Figure 2-14.

a) Wet Deposition



b) Dry Deposition

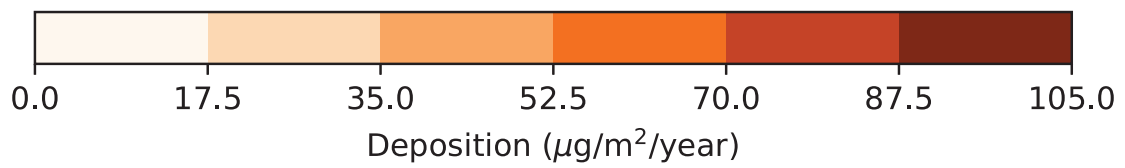
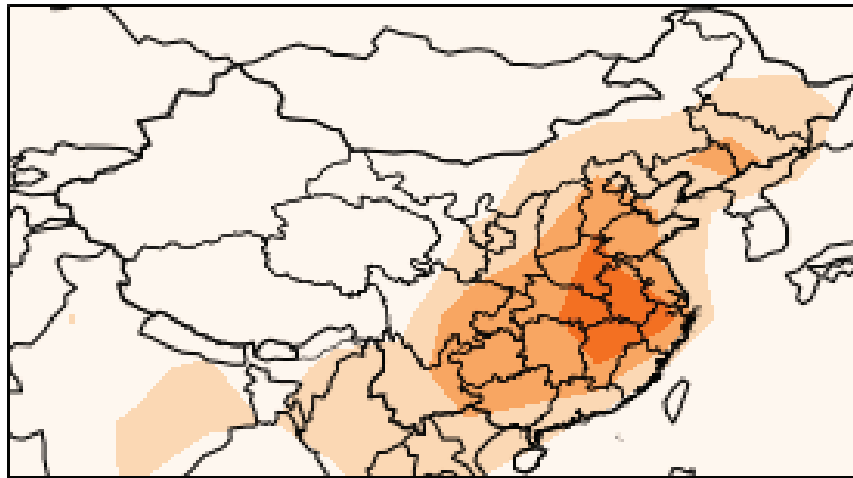


Figure 2-11: Wet and Dry Deposition, 2030 BAU Scenario

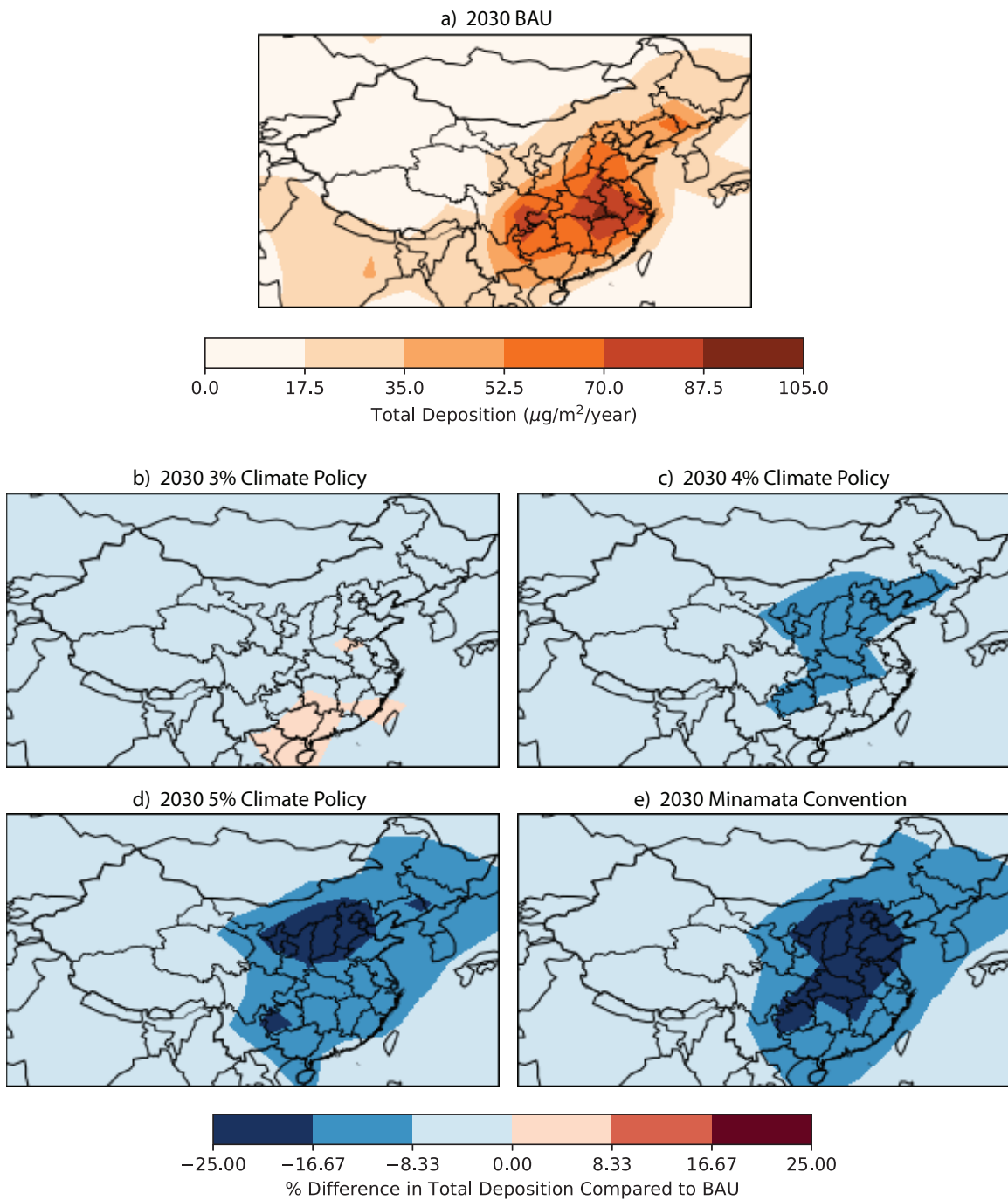


Figure 2-12: Distribution of Total Mercury Deposition in China
 (a) Absolute Total Deposition, 2030 BAU Case; (b)-(e) Reduction in Total Deposition Compared to BAU Case

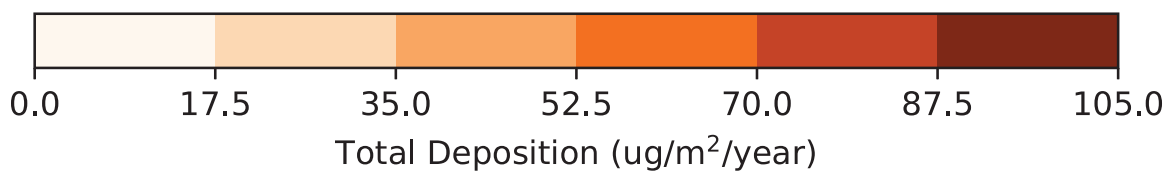
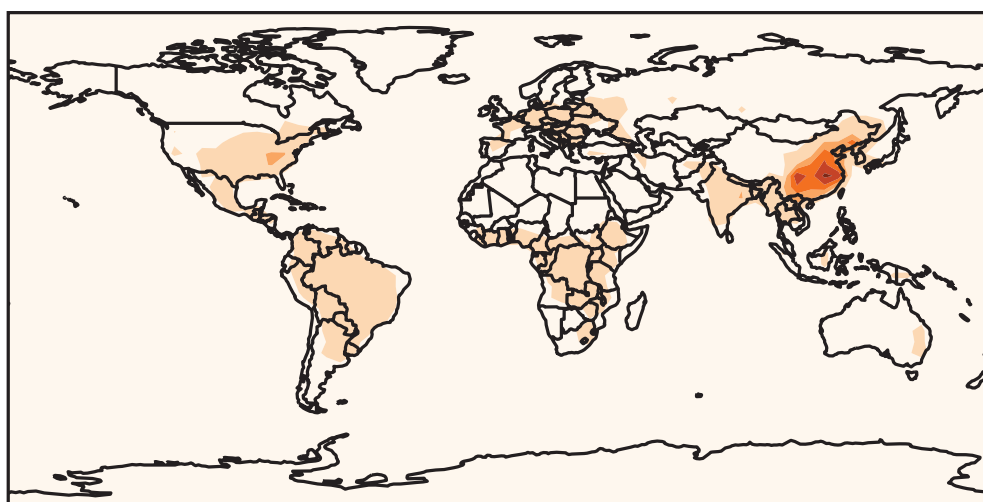
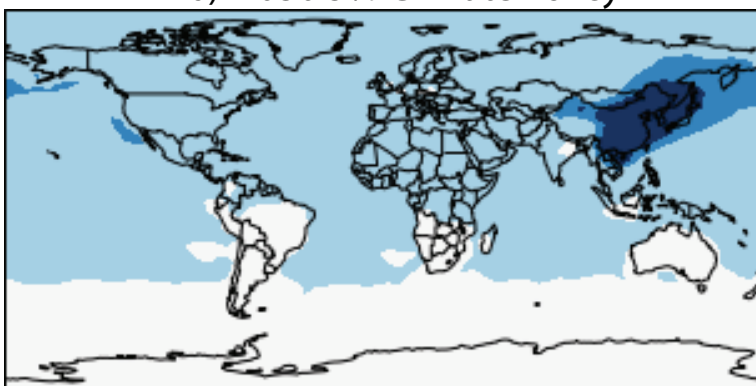


Figure 2-13: Global Total Deposition, 2030 BAU Scenario

a) 2030 4% Climate Policy



b) 2030 5% Climate Policy



c) 2030 Minamata Convention

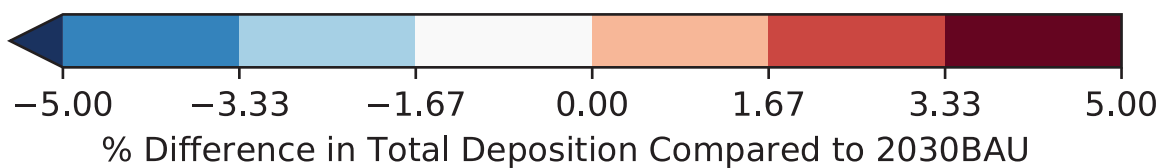
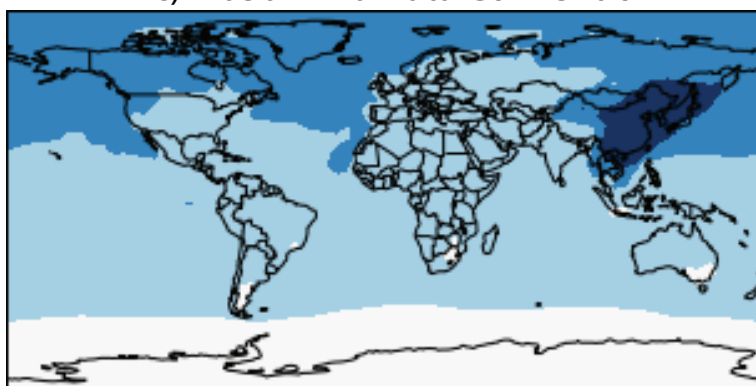


Figure 2-14: Distribution of Global Total Deposition

Table 2.13: China and the Global Mercury Budget

| | Emissions (Mg) | | | Deposition (Mg) | | | % of Global Δ Deposition |
|--------|----------------|------|----------|-----------------|------|----------|---------------------------------|
| | MC | BAU | Δ | MC | BAU | Δ | |
| Global | 4929 | 5104 | -175 | 4980 | 5154 | -174 | |
| China | 864 | 1043 | -179 | 334 | 385 | -51 | 29% |
| ROW | 4065 | 4061 | 4 | 4646 | 4769 | -123 | 71% |
| | Cint3 | BAU | Δ | Cint3 | BAU | Δ | |
| Global | 5096 | 5104 | -8 | 5146 | 5154 | -8 | |
| China | 1035 | 1043 | -8 | 382 | 385 | -3 | 38% |
| ROW | 4061 | 4061 | 0 | 4764 | 4769 | -5 | 63% |
| | Cint4 | BAU | Δ | Cint4 | BAU | Δ | |
| Global | 5022 | 5104 | -82 | 5073 | 5154 | -81 | |
| China | 959 | 1043 | -84 | 358 | 385 | -27 | 33% |
| ROW | 4063 | 4061 | 2 | 4715 | 4769 | -54 | 67% |
| | Cint5 | BAU | Δ | Cint5 | BAU | Δ | |
| Global | 4953 | 5104 | -151 | 5004 | 5154 | -150 | |
| China | 889 | 1043 | -154 | 337 | 385 | -48 | 32% |
| ROW | 4064 | 4061 | 3 | 4667 | 4769 | -102 | 68% |

ROW = rest of world MC = Minamata Convention Scenario

Cint3 = 3% Climate Policy Scenario

Cint4 = 4% Climate Policy Scenario

Cint5 = 5% Climate Policy Scenario

% of Global Δ Deposition = $\frac{Policy\Delta}{Global\Delta} * 100\%$

2.3.3 Discussion

The results of this study show that China can achieve substantial mercury emissions and deposition co-benefits through implementing national climate policy. The emissions projection results aggregated at the national level in Figure 2-4 show that all three climate policy scenarios exhibit reduced total mercury emissions ($\text{Hg}^0 + \text{Hg}^{2+} + \text{HgP}$) compared to the BAU case when aggregated to the national level, indicating the potential for substantial mercury emissions co-benefits of climate policy.

Mercury co-benefits from national climate policy could be comparable to a policy that achieves the requirements of the Minamata Convention by implementing end-of-pipe controls only. The percent reduction in mercury emissions in the 5% climate policy scenario is nearly equal to the Minamata Convention scenario (15% versus 17%, respectively). Furthermore, the maximum level of reduction in total deposition compared to the BAU case is similar in the 5% climate policy and Minamata Convention scenarios (around 25%), although the highest magnitude deposition reductions occur over a larger area in the Minamata Convention case (see Figure 2-12).

Different industries seem to bear the burden of the emissions reductions (and likely contribute differently to the deposition reductions) across the 2030 policy scenarios (see Figure 2-5). While the 3% climate policy scenario exhibits the lowest reduction in emissions compared to the BAU case, the burden of emissions reductions is most widely distributed across economic sectors in this scenario. This indicates that the carbon price acting as the policy lever in C-REM for the 3% climate policy scenario affects economic sectors evenly in comparison to the other climate policy scenarios. The distribution of the emissions reduction burden across sectors is similar in the 4% and 5% climate policy scenarios, with the Power Generation and Industry Combustion sector bearing most of the reductions. This indicates that the Power and Industry Combustion sector is most sensitive to carbon price, and the end-of-pipe controls implemented in this sector also play a role in this burden. Finally, the Power Generation and Industry Combustion sector shoulders the full burden of the emissions reduction in the Minamata Convention scenario since only end-of-pipe controls are implemented in that case.

There are some regional disparities in mercury emissions and deposition co-benefits. In general, the highest absolute levels of total emissions and deposition in 2030 occur in coastal, central, and southern provinces. In all policy scenarios, Sichuan exhibits the highest absolute level of mercury emissions, but both Sichuan and the area where Hubei, Anhui, and Jiangxi intersect exhibit the highest levels of absolute total deposition (see Figures 2-6 and 2-12). Additionally, different provinces experience the maximum level of emissions reductions compared to the BAU case across the policy scenarios (Hubei in the 3% and 5% climate policy scenarios, Shanxi in the 4% climate policy and Minamata Convention scenarios, see Figure 2-10). However, deposition reductions are small in the 3% climate policy scenario, and the maximum deposition reductions are centered over Shanxi in the 4% climate policy scenario, 5% climate policy scenario, and Minamata Convention scenario. This indicates that the provinces contributing most to emissions reductions do not necessarily see the highest decrease in total deposition.

Finally, China's emissions affect the global mercury budget. When aggregated at the global level, most mercury deposition co-benefits of climate policy in China occur outside of the country (see Table 2.13). However, I note that deposition reductions are widely distributed across the globe, so the highest magnitude reductions in deposition still occur within China for all policy scenarios (see Figure 2-14). Deposition reductions appear to stay within China in the 4% climate policy scenario and 5% climate policy scenario. Although the absolute levels of deposition reductions in China are similar between the 5% climate policy and Minamata Convention scenarios (25%, see Figure 2-12), deposition reductions outside of China are higher in the Minamata Convention scenario, indicating that the Minamata Convention scenario reduces more Hg⁰ emissions.

2.4 Policy Implications

Climate policy in China that achieves decarbonization across the country with a market-based tool such as a carbon tax can provide mercury emissions and deposition co-benefits that are comparable to policies that implement only end-of-pipe controls to meet the requirements of the Minamata Convention when aggregated to the national level. At the regional level, mercury co-benefits of climate policy are not necessarily uniform across China's provinces. Combining climate policy with end-of-pipe and process controls in areas like Sichuan could bring higher reductions in emissions and potentially deposition to this region of China. I note that the APCD technology application factors taken from Zhang et al. (2016b) are provided at the national level. Investigating APCD technologies at the province level could provide better insight into deposition interactions across provinces.

I note that the mercury emissions and deposition co-benefits observed in the climate policy scenarios are not directly additive to the Minamata Convention scenario. This is because a portion of the mercury co-benefits of climate policy are due to end-of-pipe controls compliant with existing regulations that I implement using APCD technology information from Zhang et al. (2016b). Evaluating a policy scenario that combines end-of-pipe controls compliant with the Minamata Convention, along with the benefits of decarbonizing the economy through a national climate policy like a carbon tax, would likely reveal benefits greater than either the Minamata Convention controls or the climate policy alone.

The uneven distribution of the emissions reduction burden across economic sectors and provinces indicates that harmonizing climate and Minamata Convention policy could be difficult and lead to unforeseen interactions economy-wide. Without deliberate planning or monitoring, costs of complying with climate policy and Minamata Convention policy in China could accrue unevenly in certain sectors or provinces.

The climate policy scenarios evaluated in this study specifically utilize a carbon tax for implementation across the provinces in China. I do not account for process efficiency improvements that would reduce energy use and raw materials input. Considering climate policies that use this implementation strategy would likely increase mercury emissions and deposition co-benefits. Additionally, the comparatively small

reduction in mercury emissions compared to the BAU case across climate policy options for the cement, iron and steel, non-ferrous metals production, large-scale gold mining, and waste EDGAR sectors is an artifact of the carbon tax adjustment to sector production in C-REM. This result indicates that the price on CO₂ does not have a large impact on economic output from these sectors. Sensitivity analyses examining C-REM outputs and individual sector contribution to deposition could provide greater insight into the mercury co-benefits of climate policy from these sectors.

Two principal uncertainties of the mercury biogeochemical cycle could affect my results, including in-plume reduction and the impact of legacy emissions. The chemical mechanism by which Hg⁰ is oxidized to Hg²⁺ is debated by researchers and serves as a source of uncertainty in global chemical transport models. A review completed by Ariya et al. (2015) lists oxidation reactions of mercury with NO_x (NO and NO₂), HO_x (OH and HO₂), ozone, and halogens such as bromine as having “atmospheric importance”, but that atmospheric models often simplify the chemical mechanisms. For example, the version of GEOS-Chem that I use for this analysis models Hg⁰ oxidation as a reaction with bromine in accordance with Holmes et al. (2010) (I note that I do not use GEOS-Chem with the new chemical mechanisms for mercury oxidation and reduction from Horowitz et al. (2017); they improve on the model’s halogen chemistry, including both bromine and chlorine). Previous studies have found a discrepancy between modeled and observed Hg⁰ concentrations and wet deposition fluxes (Seigneur et al., 2006; Selin et al., 2008; Holmes et al., 2010; Zhang et al., 2012; Baker & Bash, 2012; Holloway et al., 2012; Bash et al., 2014; Gustin et al., 2015; Travnikov et al., 2017). Researchers debate whether some Hg²⁺ is reduced back to Hg⁰ in the atmosphere in the aqueous phase of clouds or on the surface of particles. This occurs either by in-plume reduction near combustion sources such as power plants or reduction by organic acids (Ariya et al., 2015; Subir et al., 2012; Gustin et al., 2015; Driscoll et al., 2013). In-plume reduction can be evaluated by converting a portion of Hg²⁺ emissions from coal-fired power plants to Hg⁰ (Giang et al., 2015). This would likely result in greater deposition outside of China, since Hg⁰ has a longer lifetime than Hg²⁺.

Legacy emissions may also affect the deposition results of this analysis, although legacy impacts are minimized by evaluating deposition as a percent difference compared to a baseline policy scenario. Mercury emitted to the atmosphere cycles with terrestrial, freshwater, and ocean systems. On land, mercury is deposited through wet and dry deposition mostly as Hg²⁺ (Selin, 2009). It can be re-emitted through prompt recycling, litterfall decomposition in the soil where Hg²⁺ uptake has occurred followed by reduction to Hg⁰, or biomass burning (Selin, 2009; Driscoll et al., 2013). Mercury is incorporated into vegetation directly through “gas exchange” at plant leaves as well as absorption through roots by way of the soil (Selin, 2009). In freshwater and ocean systems, mercury is deposited through wet and dry deposition (Selin, 2009). Re-emission can occur when Hg²⁺ is reduced to Hg⁰ in the water (Selin, 2009). Ultimately, the final resting place of mercury is in deep ocean reservoirs (Selin, 2009). The lifetime of mercury against deposition in the deep ocean is on the order of thousands to tens of thousands of years as a result of this biogeochemical cycle, making legacy emissions important when considering the environmental burden of mercury

(Selin, 2009). The analysis performed by Giang et al. (2015), which evaluates mercury emissions from coal-fired power plants in China and India projected to 2050, concludes that legacy emissions could increase the difference between their evaluated policy scenarios by approximately 30%. They examine the impact of legacy emissions using the seven-box model developed by Amos et al. (2013). Legacy emissions would likely affect the results of this analysis in a similar way.

Chapter 3

Evaluating Policy for Sustainable Development in China

In 2015, the United Nations General Assembly adopted the 2030 Agenda for Sustainable Development. The Agenda includes 17 Sustainable Development Goals (shown in Figure 3-1) and 169 targets with deadlines ranging from 2020 to 2030 (UN General Assembly, 2015). Several of the goals are applicable to air pollution and climate policy.

- Goal 3: Ensure healthy lives and promote well-being for all at all ages.
- Goal 8: Promote sustained, inclusive and sustainable economic growth, full and productive employment and decent work for all.
- Goal 11: Make cities and human settlements inclusive, safe, resilient, and sustainable.
- Goal 13: Take urgent action to combat climate change and its impacts.

While the Sustainable Development Goals go a long way in providing a common framework for countries to achieve sustainability, the 2030 Agenda for Sustainable Development acknowledges that targets are designed to be achieved at the national level, and few metrics exist to evaluate prospective policy options for multiple dimensions of sustainable development simultaneously (UN General Assembly, 2015). Sub-national sustainability metrics could help evaluate policy options that provide incentive to participate in global collective action problems like climate change. In this chapter, I discuss a framework for evaluating climate policy in China at the sub-national level using the Inclusive Wealth Index, a metric of sustainability.

3.1 Background

3.1.1 History of Sustainable Development

In 1983, the World Commission on Environment and Development (WCED, also known as the Brundtland Commission) was tasked by the General Assembly of the



Figure 3-1: United Nations Sustainable Development Goals

United Nations to come up with “a global agenda for change” (WCED, 1987; Borowy, 2014). The culmination of the WCED’s work lives on in “Our Common Future”, where we find the definition of sustainable development most commonly used today: “... development that meets the needs of the present without compromising the ability of future generations to meet their own needs,” (WCED, 1987). Iris Borowy argues that while the Brundtland Commission did not necessarily produce an implementable agenda, they did start a conversation about what the concept means and how it could be achieved (Borowy, 2014).

The Brundtland Commission’s definition of sustainability gets at the issue of tradeoffs across environmental action and economic development. When outcomes across issue domains (such as environment and economics) and time horizons (meeting the needs of today’s population versus compromising on the needs of future generations) are not considered, policy options could present unintended effects for a population.

3.1.2 The Inclusive Wealth Index (IWI)

The Inclusive Wealth Index (IWI) embodies the definition set forth by the Brundtland Commission by evaluating inter-generational well-being in a country. It combines aspects of traditional economic indicators such as gross domestic product (GDP) and the Human Development Index (HDI) with measures of the natural world that influence a country’s well-being. Dasgupta (2014) describes the basis of IWI as predicated

on the Brundtland Commission’s findings.

The IWI quantifies a country’s capital stocks, including produced capital, natural capital, and human capital.

- **Produced capital** is traditional built capital assets, also described as reproducible or manufactured capital. It includes equipment, machinery, roads, and other physical infrastructure (UNU-IHDP & UNEP, 2012).
- **Natural capital** is resources derived from the natural world with use-value, aesthetic value, and cultural value. It includes fossil fuels, minerals, forest resources, agricultural land, and other ecosystem services (UNU-IHDP & UNEP, 2014).
- **Human capital** represents the value of a society’s people. It includes “education, skills, tacit knowledge, and health” (UNU-IHDP & UNEP, 2012).

Together, these capital assets represent the productive base of well-being (Dasgupta, 2014). If the value of the capital assets does not diminish over time, inter-generational well-being is maintained (Dasgupta, 2014).

3.1.3 Using IWI as a Tool for Policy Analysis

Several previous studies outline a framework for using the IWI for retrospective and prospective policy analysis.

Early IWI evaluations focused on national-level, retrospective data. Arrow et al. (2012) detailed a theoretical framework for the concept of inclusive wealth and applied it to a retrospective analysis of total produced capital, natural capital, and human capital (considering education and health) in the United States, China, India, Venezuela, and Brazil. The 2014 Inclusive Wealth Report includes a discussion on using the inclusive wealth index to assess policy instead of the capital stocks of an entire country at large (UNU-IHDP & UNEP, 2014). One of their case studies examines air pollution and energy infrastructure in China using an analysis by Matus et al. (2012). The case study raises an interesting question about China: when policy outcomes are considered in a holistic way with metrics such as the IWI, is it possible that the capital gains aimed at developing the economy can outweigh the monetized cost of environmental externalities? They use a computable general equilibrium model to internalize health benefits from reduced air pollution back into China’s economy through lost labor and leisure time from 1975 to 2005. The Inclusive Wealth Report suggests that the high magnitude increase in produced capital in China from 1975 to 2005 may actually compensate for the reductions in human capital from air pollution over the same period.

Using IWI to evaluate prospective policies requires a comparison across policy outcomes. Collins et al. (2017) present the first prospective policy analysis using the IWI. They examine 2050 electricity policy options at the national level in the oil-producing countries of Saudi Arabia, Kuwait, and the United Arab Emirates, taking into consideration produced capital, natural capital represented by oil stocks,

and human capital represented by educational attainment and applicable impacts on wages. They do not consider a health component of human capital. They find policy options that lead to reduced oil consumption can result in a net increase in inclusive wealth (incorporating human capital) for Saudi Arabia and Kuwait, but a net decrease for the United Arab Emirates.

Siddiqi & Collins (2017) argue that low spatial resolution of index results is a weakness of the Inclusive Wealth analyses performed to date. National level IWI results conceal variations in the allocation of wealth provided by the various capital stocks, making it difficult to draw conclusions on a policy’s ability to achieve inclusive growth and development (Siddiqi & Collins, 2017). Inclusive growth and development is the concept that people across the socioeconomic spectrum benefit from a changing economy where growth occurs across sectors, an idea that aligns well with the 2030 Sustainable Development Agenda intent to ensure “no one is left behind” (Siddiqi & Collins, 2017; Samans et al., 2015; UN General Assembly, 2015). Evaluating inclusive growth using IWI requires country-specific studies that capture the distributional impacts of a national policy as close to the local level as possible.

3.2 A Framework for Evaluating Climate Policy in China Using IWI

In this chapter, I suggest a framework for comparing prospective climate policies in China at the sub-national level using the IWI by drawing on the methodologies used by Arrow et al. (2012), the 2014 Inclusive Wealth Report (UNU-IHDP & UNEP, 2014), and Collins et al. (2017). I suggest utilizing provincial-level economic data from the C-REM model analysis on climate policy and PM_{2.5} co-benefits performed by Li et al. (2017b) to calculate produced capital and natural capital. I also suggest a method for incorporating high-resolution health data (1/2° × 2/3° latitude-longitude grid) into the IWI analysis. The climate policy scenarios I discuss here are from Li et al. (2017b) and are listed in Table 2.5. For a discussion of the analysis performed by Li et al. (2017b), see Chapter 2.

3.2.1 Produced Capital

The 2014 Inclusive Wealth Report defines produced capital by combining a base year of capital, investment in each year since the base year, and a capital depreciation rate (UNU-IHDP & UNEP, 2014).

$$K_t = (1 - \delta)^t K_0 + \sum_{j=1}^t I_j (1 - \delta)^{t-j} \quad (3.1)$$

where

K_t = Produced capital in the current year

δ = Capital depreciation rate

K_0 = Produced capital in the base year

I_j = investment in each year between the base year and the current year

t = current year

j = interim years between the base year and the current year

Essentially, Equation 3.1 states that produced capital in the current year is the sum of depreciated capital from the base year and new capital investments in the interim years. Taking the difference of K_t for two different policy scenarios with the same base year simplifies the data required to perform the calculation.

The economic evaluation performed by Li et al. (2017b) using C-REM analyzes 2030 policy scenarios with a base year of 2007. C-REM outputs “Total Investment in Current Value” for each province and policy scenario in the year 2030 (Springmann et al., 2015; Zhang et al., 2013, 2016a). I approximate the difference in produced capital based on the discounted difference in investment between the climate policy scenarios and the 2030 BAU case.

$$\Delta K_p = I_{p,policy}(1 - \delta)^{t-j} - I_{p,bau}(1 - \delta)^{t-j} \quad (3.2)$$

Here, p represents each province in China. I use a capital depreciation rate of 4% per year, which is aligned with the methodology of the 2014 Inclusive Wealth Report (UNU-IHDP & UNEP, 2014).

3.2.2 Natural Capital

I use fossil fuel resources to represent natural capital in China. The climate policies evaluated in Li et al. (2017b) are essentially implemented as a carbon tax, making coal resources a good indicator of changes in natural capital across the climate policy scenarios.

The 2014 Inclusive Wealth Report (UNU-IHDP & UNEP, 2014) and Arrow et al. (2012) define natural capital from fossil fuels as the product of the resource stock, production, and shadow price subtracted from fossil fuel reserves in a base year. C-REM includes estimates of the fossil fuel reserves in each province in the model’s base year, 2007. C-REM also outputs fossil fuel production for each province and policy scenario in 2030.

To find the natural capital in a future year of interest to policy, this calculation should be performed for each year between the base year and policy year. However, I estimate production in interim years between 2007 and 2030 by multiplying production in 2030 by 23 years. In the absence of data on shadow price and coal price for each province and policy scenario from Li et al. (2017b), I use the 2015 coal price in Asia from British Petroleum (2016) to approximate the 2030 price.

Change in natural capital from coal between the climate policy scenarios and the 2030 BAU case in a province of China can be calculated as follows.

$$\Delta N_{ff,p} = (S_{2007} - 23 * production_{j,p,policy}) * p_c - (S_{2007} - 23 * production_{j,p,bau}) * p_c \quad (3.3)$$

where

$\Delta N_{ff,p}$ = Difference in natural capital from fossil fuels

S_{2007} = China coal stock in C-REM's base year, 2007, mtce

$production_{j,p}$ = Production in each year between 2015 and 2030 in each province of China, mtce

p_c = Price of coal, Asia, British Petroleum (2016), \$60USD/tonne

3.2.3 Health Capital to Represent Human Capital

The component of human capital most likely affected by climate policy in China is health capital. Arrow et al. (2012) defines health capital (H) for an individual as “the expected discounted years of life remaining multiplied by the value of an additional year of life”.

$$H = \sum_{a=1}^{10} VSLY_a (L_a - A_a) (Pop_a - Mort_a) \quad (3.4)$$

$$VSLY_a = \frac{VSL_{China}}{(L_a - A_a)} \quad (3.5)$$

where

a = China's population organized into 10 age groups

$VSLY_a$ = Value of a statistical life year for the age group of interest, discounting optional

L_a = Total life expectancy of age group a (in years/life)

A_a = Average age of age group a (in years/life)

Pop_a = Population of age group a

$Mort_a$ = Mortality of age group resulting from the policy scenario of interest

VSL_{China} = China's value of a statistical life

Li et al. (2017b) calculate avoided mortality resulting from PM_{2.5} health co-benefits of climate policy using the 2010 Global Burden of Disease exposure-response relationships in a 0.25° × 0.667° latitude-longitude grid over China (Burnett et al., 2014). Health capital can be computed at this same grid resolution, and can be aggregated to the province level for comparison with produced capital and natural capital data. Here, I estimate health capital at the province level. I combine equations 3.4 and 3.5 to give a simplified form of health capital, the sum of the VSL-value of the age group populations for a given policy scenario. The difference in health capital between two policy scenarios can be calculated using mortality data from each policy scenario and combining age groups.

$$\Delta H_p = \sum_{a=1}^{10} VSL_{China} (Mort_{a,p,bau} - Mort_{a,p,policy}) \quad (3.6)$$

Li et al. (2017b) monetize health benefits using several estimations of VSL. Here, I use the VSL calculated using data for China from Wang & He (2010) converted to 2007 USD, at \$165,000 2007 USD, and no discounting. Note that the health capital calculation and subsequently the inclusive wealth index is sensitive to choice of VSL value.

3.2.4 Results

Figure 3-2 shows the change in inclusive wealth between each of the climate policy scenarios and the BAU case. In each policy scenario, Shanxi exhibits the greatest increase in Inclusive Wealth ranging from \$30 billion 2007 USD in the 3% climate policy scenario to over \$400 billion 2007 USD in the 5% climate policy scenario. Most provinces experience higher inclusive wealth in the climate policy scenarios, although there are a few provinces that have slightly higher inclusive wealth in the BAU case.

Produced capital primarily decreases in the climate policy scenarios, whereas natural capital and health capital increase across the provinces and climate policy scenarios. Shanxi exhibits the highest magnitude change in produced capital and natural capital in all climate policy scenarios, and Guangdong experiences the greatest change in health capital in all climate policy scenarios. Figures 3-3, 3-4, and 3-5 show the changes in produced capital, natural capital, and human capital, respectively, for the 4% climate policy scenario. The distribution of changes in the capital stocks is similar across policy scenarios.

3.2.5 Discussion

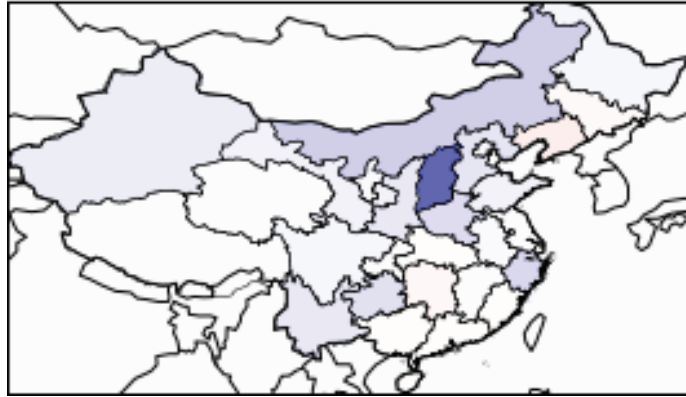
This analysis shows that the difference in Inclusive Wealth between the BAU case and climate policy scenarios in China varies across provinces (see Figure 3-2). Most provinces experience higher Inclusive Wealth under the climate policy scenarios compared to the BAU case, indicating that the climate policy scenarios could be considered more sustainable than the 2030 BAU trajectory.

Only produced capital is lower in the climate policy scenarios in some provinces compared to the BAU case, indicating that climate policy results in lower built capital stock investment. Natural capital savings in the climate policy scenarios is an order of magnitude higher than the change in either produced capital or human capital. Practically speaking in the context of this analysis, this means that China ends up with greater coal stock in the climate policy scenarios compared to the 2030 BAU case.

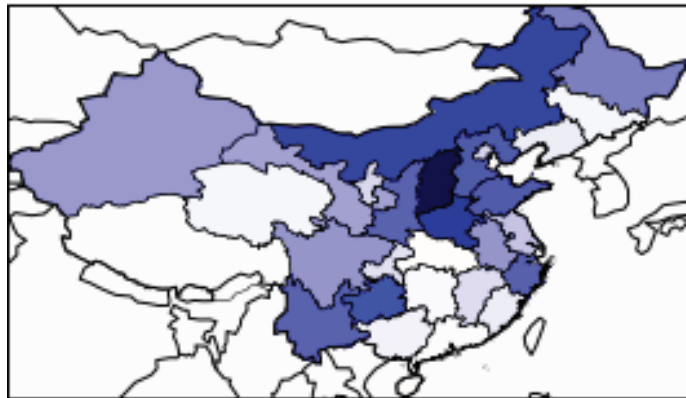
This analysis does not provide insight into the interaction between China's Inclusive Wealth and the rest of the world. Particularly, I cannot make a determination on what China might do with the additional coal stock. If they sell it to other countries, this would likely have a negative impact on health capital elsewhere in the world, but could perhaps improve produced capital assets.

I note that I do not account for trends in changing investment and coal production over time in the calculation of produced capital and natural capital, respectively. If these trends are somewhat linear or behave similarly in the climate policy scenarios

(a) 3% Climate Policy



(b) 4% Climate Policy



(c) 5% Climate Policy

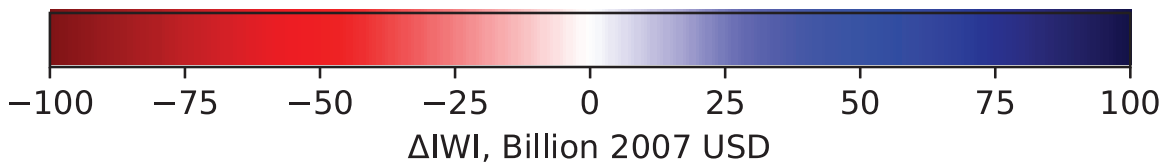
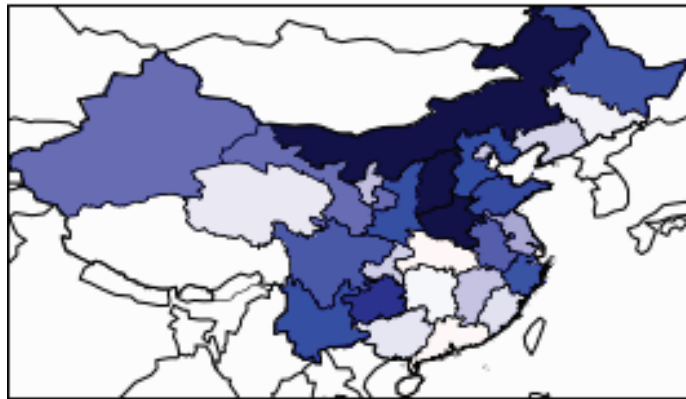


Figure 3-2: Change in Inclusive Wealth Index Compared to 2030 BAU Case

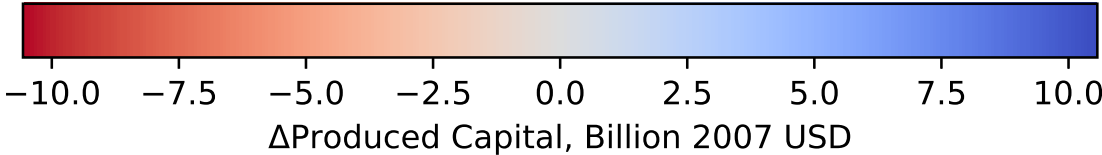
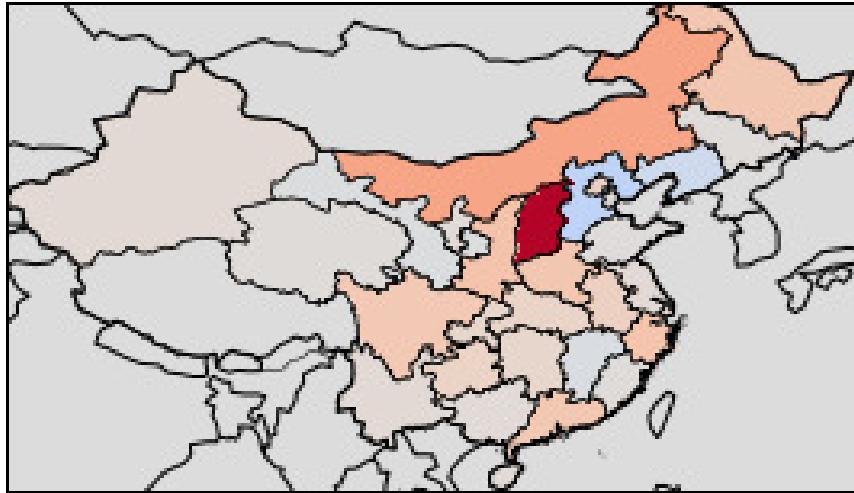


Figure 3-3: Changes in Produced Capital
4% Climate Policy Scenario Compared to 2030 BAU Case

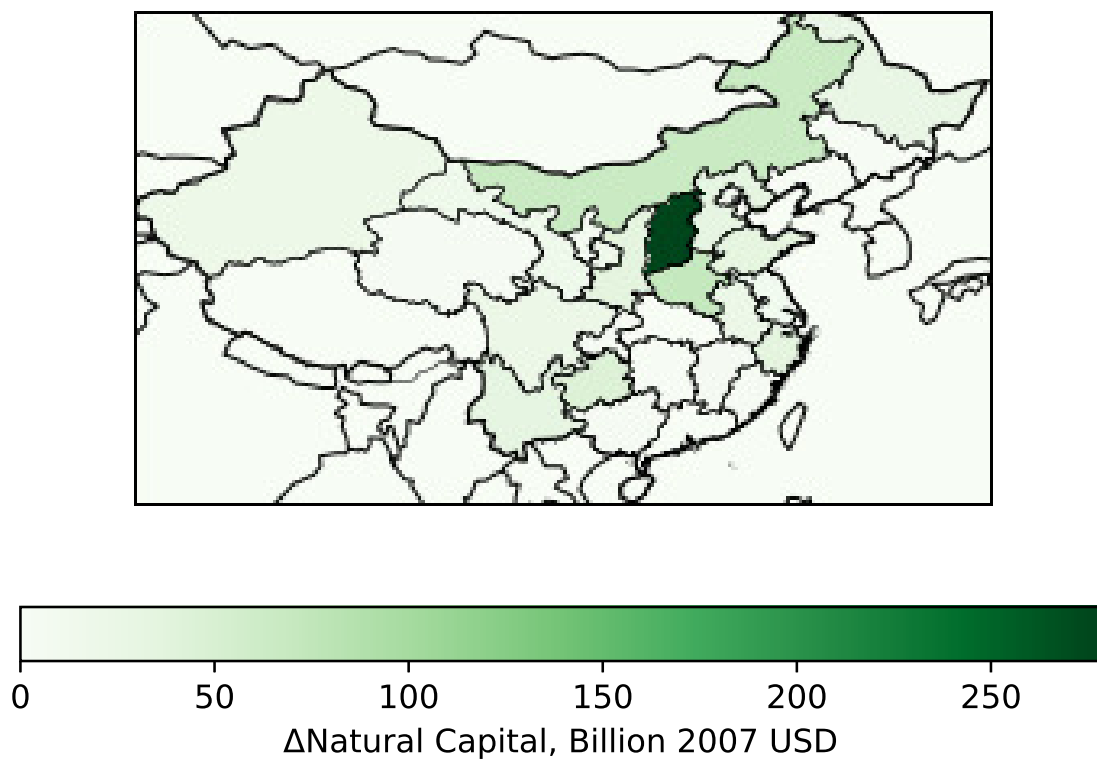


Figure 3-4: Changes in Natural Capital
4% Climate Policy Scenario Compared to 2030 BAU Case

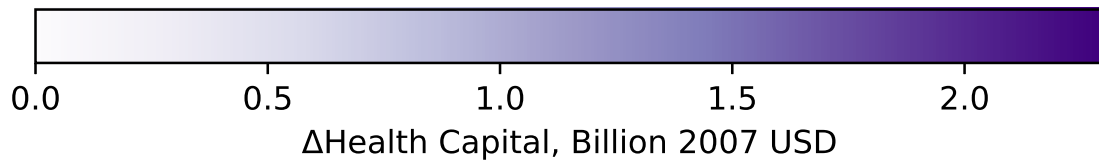
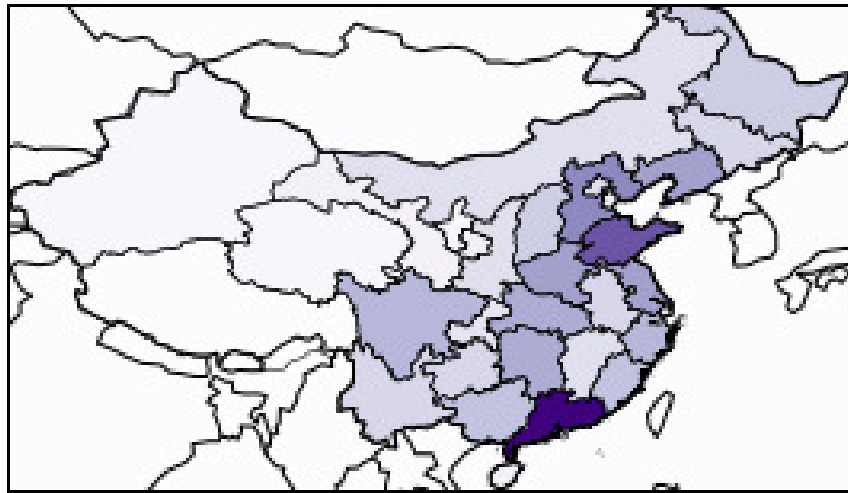


Figure 3-5: Changes in Health Capital
4% Climate Policy Scenario Compared to 2030 BAU Case

and the BAU case, then this methodology choice likely does not impact the results. However, differing trends between the climate policy scenarios and the BAU case could change the results.

Additionally, I am not using a shadow price to calculate natural capital as recommended by the 2014 Inclusive Wealth Report (UNU-IHDP & UNEP, 2014). Shadow price expresses hidden value consumers place on a good that is not expressed by market price, i.e. it is the utility value of a good (Kerr, 2015b). In the case of coal, hidden value could be tied up in its ability to provide cheap energy to a coal plant in rural China that supplies homes with reliable electricity that previously did not have access. Including shadow price in the natural capital calculation would likely increase Inclusive Wealth within a given year and policy scenario.

Overall, this framework provides an alternative method for monetizing the effect of policy options. It gives different results from evaluating gross domestic product (GDP) alone. Li et al. (2017b) provide changes in consumption across the provinces for the 4% climate policy scenario, which can serve as a proxy for GDP. With the exception of Liaoning, Hebei, Jiangxi, and Gansu, all other provinces experience a decrease in consumption in the Li et al. (2017b) study, whereas Inclusive Wealth increases in nearly all provinces based on the same set of economic output in the 4% climate policy scenario. Additionally, this framework has the flexibility to take into account more factors than a co-benefits analysis such as the one performed in Chapter 2. The following section describes how cropland and human capital effects of mercury pollution could be incorporated into this Inclusive Wealth evaluation.

3.2.6 Options for Incorporating Mercury Pollution

Cropland could also be another form of natural capital evaluated under climate policy options. In the context of China, cropland could be impacted by climate policy through mercury pollution. Rice is a possible human exposure pathway for mercury (Meng et al., 2011, 2014). In Chapter 2, I analyze the mercury co-benefits of climate policies and find that climate policy could provide substantial reductions in total mercury deposition compared to the BAU case across China. Evaluating the change in deposition over rice-growing areas in China could be included in the natural capital calculation.

The 2014 Inclusive Wealth Report defines natural capital from cropland on the basis of the crop’s average rental price per hectare, R_{pa} (UNU-IHDP & UNEP, 2014).

$$R_{pa} = \frac{RPQ}{A} \tag{3.7}$$

where

R is the rental rate of the crop

P is the price per quantity of crop

Q is the quantity of crop produced

A is the total area harvested

Mercury contamination of rice paddies could be represented in the calculation of natural capital as reduced values of A and Q . Geospatial data on rice-growing areas

overlaid with mercury deposition could determine A . Expected effects of the level of deposition on production quantity could be evaluated for Q . Future work is required to develop a framework for evaluating changes in cropland natural capital for climate policy scenarios in China on the basis of mercury contamination of rice paddies.

Additionally, long-term, low-dose health effects of methylmercury exposure through fish consumption and rice consumption could be incorporated into the human capital component of inclusive wealth. Pregnant women and their young children exposed as developing fetuses are considered the most sensitive population to mercury exposure, with exposure in utero linked to neurologic functions in children such as “cognitive development, attention and behavior, and motor skills,” (Axelrad et al., 2007). Researchers also recognize cardiovascular effects in adults as an effect of long-term, low-dose exposure to methylmercury (Roman et al., 2011). Other possible health impacts include carcinogenic, reproductive, and immunological effects (Yorifuji et al., 2013; NRC, 2000).

The neurologic effects of mercury could contribute to components of human capital besides health, including education, skills, and lifetime earnings. Other health effects of mercury could be incorporated as health capital, similar to the evaluation of $PM_{2.5}$ health effects provided above. This would require analysis of fish tissue and rice plant concentration changes with the policy scenarios, and corresponding dietary data for the affected population, in addition to an atmospheric fate and transport analysis such as the one performed in Chapter 2 (Giang & Selin, 2016). However, data on fish tissue concentration for seafood consumed in China, rice plant concentrations, and Chinese population dietary data are not currently available.

Chapter 4

Policy Recommendations and Conclusions

In this chapter, I consider my final research question on how decision-makers can consider interacting factors of climate change, air pollution, and economic development in evaluating regional effects of national-level policy options that address international commitments.

4.1 Taking Action on Climate Change and Meeting Environmental Goals Effectively

The results of the mercury co-benefits study presented in Chapter 2 show that China has policy options for addressing climate change and mercury pollution simultaneously. The flexibility already exists within the Paris Agreement on climate change and the Minamata Convention on Mercury to design implementation strategies that utilize co-benefits. As discussed in Chapter 1, countries are free to create their own NDCs tailored to their domestic needs under the Paris Agreement. Similarly, the Minamata Convention directs Parties to create a National Implementation Plan to control emissions. Multi-pollutant control strategies that take advantage of co-benefits are included in the list of measures countries can choose from for controlling emissions from existing sources. A National Implementation Plan taking advantage of mercury co-benefits of climate policy would thus fall under the requirements of the Minamata Convention on Mercury.

Furthermore, the international environmental governance community has already recognized the link between climate change and other forms of pollution within the framework of the Montreal Protocol on Substances that Deplete the Ozone Layer. Negotiators recently provided a new motivator for chemical companies to develop alternatives to hydrofluorocarbons (HFCs), gases with high global warming potential relative to CO₂. HFCs became the primary replacement for chlorofluorocarbons (CFCs), substances commonly used for refrigeration and air conditioning that were shown to deplete the ozone layer (Deol et al., 2015; Solomon, 1999). In October 2016, at the 28th Meeting of the Parties to the Montreal Protocol, the member par-

ties adopted the Kigali amendments to phase-down HFCs on the basis of their global warming potential, although climate change was not the original focus of the Protocol (UNEP, 2016b).

4.2 Sustainable Development and Meeting Environmental Goals Effectively

The analysis presented in Chapter 2 finds substantial reductions in mercury deposition for the 4% and 5% Climate Policy scenarios compared to the BAU case. However, this environmental indicator taken by itself does not tell the full story of mercury co-benefits in the country because we cannot draw conclusions about the impact of mercury and climate policy on human health from deposition data alone.

Humans are primarily exposed to mercury through seafood consumption. Mercury combines with a methyl group (CH_3^+) in the environment to form methylmercury, a compound that is particularly harmful to humans (Selin, 2009). According to Selin (2009), methylmercury is a neurotoxin that “accumulates through multiple levels in the aquatic food chain” (Selin, 2009). This means that aquatic predators consume food contaminated with methylmercury, concentrating the amount of the substance in the predator’s tissues (Selin, 2009). As a result, humans can consume methylmercury by eating contaminated fish (Selin, 2009).

Another possible human exposure pathway is through rice consumption. Methylmercury in soil is absorbed by plant roots, transferred first to the leaf and stalk, and then to the rice seed during the growing season (Meng et al., 2011). Once ripened, Meng et al. (2014) have postulated that methylmercury is incorporated into the inedible hull, edible bran, and edible white rice of the plant grain.

The accumulation of methylmercury in fish and rice is nonlinear, and the corresponding physiological response in humans to methylmercury from food consumption is also nonlinear. Furthermore, a person’s diet also influences mercury exposure, and certain demographic populations may be particularly vulnerable to exposure such as subsistence fishing and rice farming communities living below the poverty level nearby a coal-fired power plant. As a result, examining geospatial deposition data does not capture enough information on nonlinearities of human exposure to mercury, environmental justice issues associated with various policy scenarios and the status quo, and distributional effects of policy benefits to draw robust conclusions about health effects of mercury. However, understanding the health effects of mercury is vitally important.

The two most prominent high-dose methylmercury exposure episodes occurred in Japan in the 1950s and 1960s (Minamata and Niigata) and Iraq in the 1970s (Yorifuji et al., 2013). Chemical manufacturers Chisso (with a factory in Minamata) and Showa Denko (with a factory in Niigata) released methylmercury associated with manufacture of acetaldehyde into local waterways, contaminating seafood consumed by residents (Yorifuji et al., 2013). In Iraq, mercury used in fungicides in the 1970s contaminated mislabeled seed grains meant for making bread (Yorifuji et al., 2013).

The health impacts resulting from these high exposure episodes served as a motivator for controlling mercury releases to the environment. The symptoms of human MeHg exposure in these two cases included difficulty walking and speaking, loss of peripheral vision, and impaired hearing (Yorifuji et al., 2013). Additionally, children in Minamata, Japan, born to mothers who had consumed large doses of methylmercury while they were pregnant exhibited intellectual disabilities, reduced motor skills and reflexes, physical deformities, and impaired growth (Yorifuji et al., 2013). Over 2000 people are officially diagnosed with Minamata disease from the exposure incidents in Japan, while tens of thousands exhibit some of these neurological symptoms characteristic of a high-dose methylmercury exposure (Yorifuji et al., 2013). The Iraq exposure episode likely resulted in thousands of hospitalizations and hundreds of deaths (Yorifuji et al., 2013).

As a result of the high-dose methylmercury exposure episodes, scientists and policymakers now consider the effects of long-term, low-dose human exposure to methylmercury. Pregnant women and their young children exposed as developing fetuses are considered the most sensitive population, with exposure in utero linked to neurologic functions in children such as “cognitive development, attention and behavior, and motor skills,” (Axelrad et al., 2007). Researchers also recognize cardiovascular effects in adults as an effect of long-term, low-dose exposure to methylmercury (Roman et al., 2011). Other possible health impacts include carcinogenic, reproductive, and immunological effects (Yorifuji et al., 2013; NRC, 2000).

In addition to the severity of mercury exposure effects on individuals, monetizing health effects shows that human exposure to mercury can present a significant economic burden to a society as a whole. Giang & Selin (2016) performed a comprehensive analysis of the health benefits associated with several policy scenarios controlling mercury emissions in the United States. The policy scenarios are based on the Mercury and Air Toxics Standards as well as the US commitments under the Minamata Convention on Mercury. They monetize IQ effects in children and cardiovascular effects in adults on an economy-wide basis (accounting for labor productivity and wages) and a lifetime basis (“cost-of-illness and value of a statistical life”). They estimate that the more stringent mercury control scenario based on the Minamata Convention results in monetized economy-wide welfare benefits of \$43 billion to \$104 billion and \$147 billion to \$339 billion in lifetime welfare benefits.

A health impact analysis like the one performed by Giang & Selin (2016) requires atmospheric analyses on the fate and transport of mercury, analysis on fish tissue concentration changes with the policy scenarios, and corresponding dietary data for the affected population. The analysis performed in Chapter 2 could serve as the atmospheric fate and transport input to an evaluation of mercury health impacts in China. However, data on fish tissue concentration for seafood consumed in China and Chinese population dietary data are not currently available.

Another dimension of health impact analysis of mercury exposure in China could focus on rice consumption. Few studies have focused on human exposure to mercury through rice. Deposition results from the evaluation in Chapter 2 performed at a higher spatial resolution could support a framework to evaluate human exposure to mercury through rice consumption in China, combined with data on rice crop

production, dietary data, and rice plant concentrations of mercury.

A health impact analysis on mercury exposure through fish and rice consumption in China could contribute to a more comprehensive analysis of inclusive wealth, especially for the health capital component of the index. The 2014 Inclusive Wealth report states that, “[Health capital] is likely the most important form of capital in producing human well-being,” (UNU-IHDP & UNEP, 2014). Capturing multiple dimensions of human health through health capital could help make the IWI a more robust indicator of sustainable policy options.

The health effects of China’s mercury emissions do not halt at China’s borders. China’s domestic mercury and mercury policy influence human and ecosystem exposure not only within the country’s borders, but also in the world’s oceans, exerting influence on mercury contamination of the global seafood market. Giang et al. (2015) project emissions from coal-fired power plants to 2050 in China and India under Minamata Convention policy scenarios and find that deposition benefits are significant to the Pacific and Indian Oceans, major sources of seafood to the world market. In a later study focused on mercury emissions in the US, Giang & Selin (2016) reach a similar conclusion on deposition in the Pacific and Atlantic oceans, where much of the US commercial fish market sources its product. They find that deposition to these oceans is “heavily influenced by emissions from non-US sources, including East and South Asia,” (Giang & Selin, 2016).

4.3 Incentive for Collective Action

The crux of the analyses performed in this thesis is that local air pollution co-benefits and a holistic examination of factors contributing to sustainable environmental policy could provide incentive for collective action on global issues such as climate change. Specifically, mercury co-benefits of climate policy in China can be realized within the country as well as the rest of the world. This dual international and local behavior of mercury, and its interactions with climate policy, makes it a prime issue to straddle the massive collective action challenge of international environmental governance discussed in Chapter 1. In particular, the 5% climate policy scenario provides China with perhaps the greatest incentive to participate in collective action on climate change. This climate policy option is ambitious for China as it would reduce their carbon intensity to the global mean level by 2030. Under this policy scenario, the country can take advantage of domestic mercury co-benefits that help remedy international mercury pollution while also meeting its commitments to global climate action. Additionally, this policy option shows the highest level of Inclusive Wealth compared to a business-as-usual trajectory. Regardless of their policy choice, China’s commitments under the Paris Agreement and Minamata Convention are linked with the rest of the world, and their continued involvement in international environmental governance is crucial.

Bibliography

- Allison, G. T. (1969). Conceptual Models and the Cuban Missile Crisis. *The American Political Science Review*, 63(3), 689–718.
- Amos, H. M., Jacob, D. J., Holmes, C. D., Fisher, J. A., Wang, Q., Yantosca, R. M., Corbitt, E. S., Galarneau, E., Rutter, A. P., Gustin, M. S., Steffen, A., Schauer, J. J., Graydon, J. A., St Louis, V. L., Talbot, R. W., Edgerton, E. S., Zhang, Y., & Sunderland, E. M. (2012). Gas-particle partitioning of atmospheric Hg(II) and its effect on global mercury deposition. *Atmospheric Chemistry and Physics*, 12, 591–603.
- Amos, H. M., Jacob, D. J., Streets, D. G., & Sunderland, E. M. (2013). Legacy impacts of all-time anthropogenic emissions on the global mercury cycle. *Global Biogeochemical Cycles*, 27, 410–421.
- Ariya, P. A., Amyot, M., Dastoor, A., Deeds, D., Feinberg, A., Kos, G., Poulain, A., Ryjkov, A., Semeniuk, K., Subir, M., & Toyota, K. (2015). Mercury Physicochemical and Biogeochemical Transformation in the Atmosphere and at Atmospheric Interfaces: A Review and Future Directions. *Chemical Reviews*, 115, 3760–3802.
- Arrow, K. J., Dasgupta, P., Goulder, L. H., Mumford, K. J., & Oleson, K. (2012). Sustainability and the Measurement of Wealth. *Environment and Development Economics*, 17, 317–353.
- Axelrad, D. A., Bellinger, D. C., Ryan, L. M., & Woodruff, T. J. (2007). Dose-Response Relationship of Prenatal Mercury Exposure and IQ: An Integrative Analysis of Epidemiologic Data. *Environmental Health Perspectives*, 115(4), 609–615.
- Baker, K. R., & Bash, J. O. (2012). Regional scale photochemical model evaluation of total mercury wet deposition and speciated ambient mercury. *Atmospheric Environment*, 49, 151–162.
- Bash, J. O., Carlton, A. G., Hutzell, W. T., & Bullock, O. R. (2014). Regional air quality model application of the aqueous-phase photo reduction of atmospheric oxidized mercury by dicarboxylic acids. *Atmosphere*, 5, 1–15.
- Bey, I., Jacob, D. J., Yantosca, R. M., Logan, J. A., Field, B. D., Fiore, A. M., Li, Q.-B., Liu, H.-Y., Mickley, L. J., & Schultz, M. G. (2001). Global Modeling of Tropospheric Chemistry with Assimilated Meteorology: Model Description and Evaluation. *Journal of Geophysical Research*, 106(D19), 23073–23095.

- Borowy, I. (2014). *Defining Sustainable Development for Our Common Future*. London and New York: Routledge.
- British Petroleum (2016). BP Statistical Review of World Energy. Tech. rep.
 URL <https://www.bp.com/content/dam/bp/pdf/energy-economics/statistical-review-2016/bp-statistical-review-of-world-energy-2016-full-report.pdf>
- Burnett, R. T., Arden Pope, C., Ezzati, M., Olives, C., Lim, S. S., Mehta, S., Shin, H. H., Singh, G., Hubbell, B., Brauer, M., Ross Anderson, H., Smith, K. R., Balmes, J. R., Bruce, N. G., Kan, H., Laden, F., Prüss-Ustün, A., Turner, M. C., Gapstur, S. M., Diver, W. R., & Cohen, A. (2014). An integrated risk function for estimating the global burden of disease attributable to ambient fine particulate matter exposure. *Environmental Health Perspectives*, *122*(4), 397–403.
- Chen, C., Wang, H., Zhang, W., Hu, D., Chen, L., & Wang, X. (2013). High-resolution inventory of mercury emissions from biomass burning in China for 2000-2010 and a projection for 2020. *Journal of Geophysical Research Atmospheres*, *118*, 12248–12256.
- Cifuentes, L., Borja-Aburto, V., Gouveia, N., Thurston, G., & Davis, D. (2001). Hidden health benefits of greenhouse gas mitigation. *Science*, *293*(5533), 1257–1259.
- Climate Interactive (2017). Climate Scoreboard.
 URL <https://www.climateinteractive.org/programs/scoreboard/>
- Collins, R. D., Selin, N. E., de Weck, O. L., & Clark, W. C. (2017). Using Inclusive Wealth for Policy Evaluation: Application to Electricity Infrastructure Planning in Oil-Exporting Countries. *Ecological Economics*, *133*, 23–34.
- Corbitt, E. S., Jacob, D. J., Holmes, C. D., Streets, D. G., & Sunderland, E. M. (2011). Global source-receptor relationships for mercury deposition under present-day and 2050 emissions scenarios. *Environmental Science and Technology*, *45*, 10477–10484.
- Dasgupta, P. (2014). Measuring the Wealth of Nations. *Annual Review of Resource Economics*, *6*, 17–31.
- Davis, J. H., & Davenport, C. (2015). China to Announce Cap-and-Trade Program to Limit Emissions.
 URL <https://www.nytimes.com/2015/09/25/world/asia/xi-jinping-china-president-obama-summit.html>
- Deol, B., Anderson, S. O., Chaturvedi, V., Jaiswal, A., & Dilley, S. M. (2015). Amending the Montreal Protocol. Tech. rep., Council on Energy, Environment, and Water; Institute for Governance & Sustainable Development, Natural Resources Defense Council.

- URL <http://conf.montreal-protocol.org/meeting/mop/mop-27/pubs/ObserverPublications/AmendingtheMontrealProtocol.pdf>
- Dong, H., Dai, H., Dong, L., Fujita, T., Geng, Y., Klimont, Z., Inoue, T., Bunya, S., Fujii, M., & Masui, T. (2015). Pursuing air pollutant co-benefits of CO₂ mitigation in China: A provincial leveled analysis. *Applied Energy*, *144*, 165–174.
- Driscoll, C. T., Mason, R. P., Chan, H. M., Jacob, D. J., & Pirrone, N. (2013). Mercury as a Global Pollutant: Sources, Pathways, and Effects. *Environmental Science & Technology*, *47*, 4967–4983.
- Ellerman, A. D., Joskow, P. L., & Harrison, D. (2003). Emissions Trading in the US. Tech. rep., Pew Center on Global Climate Change.
URL <http://web.mit.edu/globalchange/www/PewCtr{ }MIT{ }Rpt{ }Ellerman.pdf>
- European Commission (2014). Global Emissions EDGARv4.tox1.
URL <http://edgar.jrc.ec.europa.eu/overview.php?v=4tox1>
- Giang, A., & Selin, N. E. (2016). Benefits of Mercury Controls for the United States. *Proceedings of the National Academy of Sciences of the United States of America*, *113*(2), 286–291.
- Giang, A., Stokes, L. C., Streets, D. G., Corbitt, E. S., & Selin, N. E. (2015). Impacts of the minamata convention on mercury emissions and global deposition from coal-fired power generation in Asia. *Environmental Science and Technology*, *49*(9), 5326–5335.
- Gustin, M. S., Amos, H. M., Huang, J., Miller, M. B., & Heidecorn, K. (2015). Measuring and Modeling Mercury in the Atmosphere: a Critical Review. *Atmospheric Chemistry and Physics*, *15*, 5697–5713.
- Hilton, I., & Kerr, O. (2017). The Paris Agreement: China’s ‘New Normal’ Role in International Climate Negotiations. *Climate Policy*, *17*(1), 48–58.
- Holloway, T., Voigt, C., Morton, J., Spak, S. N., Rutter, A. P., & Schauer, J. J. (2012). An assessment of atmospheric mercury in the Community Multiscale Air Quality (CMAQ) model at an urban site and a rural site in the Great Lakes Region of North America. *Atmospheric Chemistry and Physics*, *12*, 7117–7133.
- Holmes, C. D., Jacob, D. J., Corbitt, E. S., Mao, J., Yang, X., Talbot, R., & Slemr, F. (2010). Global atmospheric model for mercury including oxidation by bromine atoms. *Atmospheric Chemistry and Physics*, *10*, 12037–12057.
- Horowitz, H. M., Jacob, D. J., Amos, H. M., Streets, D. G., & Sunderland, E. M. (2014). Historical mercury releases from commercial products: Global environmental implications. *Environmental Science and Technology*, *48*, 10242–10250.

- Horowitz, H. M., Jacob, D. J., Zhang, Y., Dibble, T. S., Slemr, F., Amos, H. M., Schmidt, J. A., Corbitt, E. S., Marais, E. A., & Sunderland, E. M. (2017). A new mechanism for atmospheric mercury redox chemistry: Implications for the global mercury budget. *Atmospheric Chemistry and Physics, Discussions*.
- Houghton, J., Jenkins, G., & Ephraums, J. (1990). *Climate Change: the IPCC Scientific Assessment*. Cambridge: Cambridge University Press.
- IISD (2013). Summary of the Diplomatic Conference of Plenipotentiaries on the Minamata Convention on Mercury and Its Preparatory Meeting. *Earth Negotiations Bulletin, International Institute for Sustainable Development (IISD) Reporting Services*, 28(27).
- IISD (2015). Summary of the Paris Climate Change Conference. *Earth Negotiations Bulletin, International Institute for Sustainable Development (IISD) Reporting Services*, 12(663).
- IPCC (1990). *Climate Change: the IPCC Response Strategies*. World Meteorological Organization/United Nations Environment Program.
- IPCC (1996). Reporting Instructions. In *Revised 1996 IPCC Guidelines for National Greenhouse Gas Inventories*, vol. 1, chap. Volume 1, (p. 22). Task Force on National Greenhouse Gas Inventories.
- Jacob, D. J. (1999). *Introduction to Atmospheric Chemistry*. Princeton, NJ: Princeton University Press.
- Jacob, D. J. (2016). Biogeochemical Cycle of Mercury, EPS 200 Lecture, Harvard University.
- Kai, M. (2006). The 11th Five-Year Plan: Targets, Paths and Policy Orientation. URL http://en.ndrc.gov.cn/newsrelease/200603/t20060323_{_}63813.html
- Keller, C. A., Long, M. S., Yantosca, R. M., Da Silva, A. M., Pawson, S., & Jacob, D. J. (2014). HEMCO v1.0: A versatile, ESMF-compliant component for calculating emissions in atmospheric models. *Geoscientific Model Development*, 7, 1409–1417.
- Keqiang, L. (2016). Full Text: Report on the Work of the Government. URL http://www.china.org.cn/china/NPC_{_}CPPCC_{_}2016/2016-03/18/content_{_}38056401.htm
- Kerr, S. P. (2015a). MIT Course 14.030, Lecture Note 13: Externalities, the Coase Theorem and Market Remedies.
- Kerr, S. P. (2015b). MIT Course 14.030, Lecture Note 4: Theory of Choice and Individual Demand.

- Kerr, S. P. (2015c). MIT Course 14.030, Lecture Note 9: General Equilibrium in a Pure Exchange Economy.
- Li, J. S., Chen, B., Chen, G. Q., Wei, W. D., Wang, X. B., Ge, J. P., Dong, K. Q., Xia, H. H., & Xia, X. H. (2017a). Tracking mercury emission flows in the global supply chains: A multi-regional input-output analysis. *Journal of Cleaner Production*, *140*, 1470–1492.
- Li, M., Li, C.-T., Zhang, D., Mulvaney, K. M., Selin, N. E., & Karplus, V. J. (2017b). Air Quality Co-Benefits of Climate Policy in China. *Submitted to Nature Climate Change*.
- Lin, Y., Wang, S., Steindal, E. H., Wang, Z., Braaten, H. F. V., Wu, Q., & Larssen, T. (2017). A Holistic Perspective Is Needed To Ensure Success of Minamata Convention on Mercury. *Environmental Science & Technology*, *51*, 1070–1071.
- Liu, H., Jacob, D. J., Bey, I., & Yantosca, R. M. (2001). Constraints from ²¹⁰Pb and ⁷Be on wet deposition and transport in a global three-dimensional chemical tracer model driven by assimilated meteorological fields. *Journal of Geophysical Research*, *106*(D11), 12109–12128.
- Matus, K., Nam, K.-M., Selin, N. E., Lamsal, L. N., Reilly, J. M., & Paltsev, S. (2012). Health Damages from Air Pollution in China. *Global Environmental Change*, *22*, 55–66.
- Meng, B., Feng, X., Qiu, G., Anderson, C. W. N., Wang, J., & Zhao, L. (2014). Localization and Speciation of Mercury in Brown Rice with Implications for Pan-Asian Public Health. *Environmental Science & Technology*, *48*, 7974–7981.
- Meng, B., Feng, X., Qiu, G., Liang, P., Li, P., Chen, C., & Shang, L. (2011). The process of methylmercury accumulation in rice (*Oryza sativa* L.). *Environmental Science & Technology*, *45*, 2711–2717.
- Munnings, C., Morgenstern, R., Wang, Z., & Liu, X. (2014). Assessing the Design of Three Pilot Programs for Carbon Trading in China. Tech. rep., Resources for the Future.
URL <http://www.rff.org/files/sharepoint/WorkImages/Download/RFF-DP-14-36.pdf>
- Muntean, M., Janssens-Maenhout, G., Song, S., Selin, N. E., Olivier, J. G. J., Guizzardi, D., Maas, R., & Dentener, F. (2014). Trend analysis from 1970 to 2008 and model evaluation of EDGARv4 global gridded anthropogenic mercury emissions. *Science of the Total Environment*, *494-495*, 337–350.
- Nam, K.-M., Waugh, C. J., Paltsev, S., Reilly, J. M., & Karplus, V. J. (2013). Carbon co-benefits of tighter SO₂ and NO_x regulations in China. *Global Environmental Change*, *23*, 1648–1661.

- NDRC (2015). China's Intended Nationally Determined Contribution.
URL <http://www4.unfccc.int/ndcregistry/Pages/Home.aspx>
- Nielsen, C. P., & Ho, M. S. (2013). *Clearer Skies Over China*. Cambridge, Mass.: The MIT Press.
- NRC (2000). *Toxicological Effects of Methylmercury*. Washington, D.C.: National Academy Press.
- Olson, M. (1982). *The Rise and Decline of Nations*. New Haven: Yale University Press.
- Pachauri, R., Meyer, L., & IPCC Synthesis Report Core Writing Team (2014). Climate Change 2014: Synthesis Report. Tech. rep., Intergovernmental Panel on Climate Change, Geneva, Switzerland.
URL <http://www.ipcc.ch/report/ar5/syr/>
- Pacyna, E. G., Pacyna, J. M., Sundseth, K., Munthe, J., Kindbom, K., Wilson, S., Steenhuisen, F., & Maxson, P. (2010). Global emission of mercury to the atmosphere from anthropogenic sources in 2005 and projections to 2020. *Atmospheric Environment*, *44*, 2487–2499.
- Pacyna, J. M., Travnikov, O., De Simone, F., Hedgecock, I. M., Sundseth, K., Pacyna, E. G., Steenhuisen, F., Pirrone, N., Munthe, J., & Kindbom, K. (2016). Current and future levels of mercury atmospheric pollution on a global scale. *Atmospheric Chemistry and Physics*, *16*, 12495–12511.
- Putnam, R. D. (1988). Diplomacy and Domestic Politics: the Logic of Two-Level Games. *International Organization*, *42*(3), 427–460.
- Rafaj, P., Bertok, I., Cofala, J., & Schopp, W. (2013). Scenarios of Global Mercury Emissions from Anthropogenic Sources. *Atmospheric Environment*, *79*, 472–479.
- Rafaj, P., Cofala, J., Kuenen, J., Wyrwa, A., & Zysk, J. (2014). Benefits of European climate policies for mercury air pollution. *Atmosphere*, *5*, 45–59.
- Roman, H. A., Walsh, T. L., Coull, B. A., Dewailly, É., Guallar, E., Hattis, D., Mariën, K., Schwartz, J., Stern, A. H., Virtanen, J. K., & Rice, G. (2011). Evaluation of the Cardiovascular Effects of Methylmercury Exposures: Current Evidence Supports Development of a Dose-Response Function for Regulatory Benefits Analysis. *Environmental Health Perspectives*, *119*(5), 607–614.
- Samans, R., Blanke, J., Corrigan, G., & Drzeniek, M. (2015). *Insight Report: The Inclusive Growth and Development Report 2015*. World Economic Forum.
- Schuman, S., & Lin, A. (2012). China's Renewable Energy Law and its Impact on Renewable Power in China. *Energy Policy*, *51*, 89–109.

- Seigneur, C., Vijayaraghavan, K., & Lohman, K. (2006). Atmospheric mercury chemistry: Sensitivity of global model simulations to chemical reactions. *Journal of Geophysical Research Atmospheres*, *111*, 1–17.
- Selin, H. (2014). Global Environmental Law and Treaty-Making on Hazardous Substances: the Minamata Convention and Mercury Abatement. *Global Environmental Politics*, *14*(1), 1–19.
- Selin, N. E. (2009). Global Biogeochemical Cycling of Mercury: A Review. *Annual Review of Environment and Resources*, *34*(1), 43–63.
- Selin, N. E., Jacob, D. J., Yantosca, R. M., Strode, S., Jaeglé, L., & Sunderland, E. M. (2008). Global 3-D land-ocean-atmosphere model for mercury: Present-day versus preindustrial cycles and anthropogenic enrichment factors for deposition. *Global Biogeochemical Cycles*, *22*, 1–13.
- Shih, Y. H., & Tseng, C. H. (2015). Co-Benefits of Mercury Reduction in Taiwan: a Case Study of Clean Energy Development. *Sustainability Science*, *10*, 61–73.
- Siddiqi, A., & Collins, R. D. (2017). Sociotechnical systems and sustainability: current and future perspectives for inclusive development. *Current Opinion in Environmental Sustainability*, *24*, 7–13.
- Silva, R. A., West, J. J., Lamarque, J. F., Shindell, D. T., Collins, W. J., Dalsoren, S., Faluvegi, G., Folberth, G., Horowitz, L. W., Nagashima, T., Naik, V., Rumbold, S. T., Sudo, K., Takemura, T., Bergmann, D., Cameron-Smith, P., Cionni, I., Doherty, R. M., Eyring, V., Josse, B., MacKenzie, I. A., Plummer, D., Righi, M., Stevenson, D. S., Strode, S., Szopa, S., & Zengast, G. (2016). The effect of future ambient air pollution on human premature mortality to 2100 using output from the ACCMIP model ensemble. *Atmospheric Chemistry and Physics*, *16*(15), 9847–9862.
- Soerensen, A. L., Sunderland, E. M., Holmes, C. D., Jacob, D. J., Yantosca, R. M., Skov, H., Christensen, J. H., Strode, S. A., & Mason, R. P. (2010). An improved global model for air-sea exchange of mercury: High concentrations over the North Atlantic. *Environmental Science and Technology*, *44*, 8574–8580.
- Solomon, S. (1999). Stratospheric ozone depletion: A review of concepts and history. *Reviews of Geophysics*, *37*(3), 275–316.
- Springmann, M., Zhang, D., & Karplus, V. J. (2015). Consumption-based adjustment of emissions-intensity targets: An Economic Analysis for China’s Provinces. *Environmental and Resource Economics*, *61*, 615–640.
- Sterman, J. D., Fiddaman, T., Franck, T., Jones, A., Mccauley, S., Rice, P., Sawin, E., & Siegel, L. (2013). Management Flight Simulators to Support Climate Negotiations. *Environmental Modelling and Software*, *44*, 122–135.

- Stokes, L. C., Giang, A., & Selin, N. E. (2016). Splitting the South: China and India's Divergence in International Environmental Negotiations. *Global Environmental Politics*, 16(4), 12–31.
- Streets, D. G., Hao, J., Wu, Y., Jiang, J., Chan, M., Tian, H., & Feng, X. (2005). Anthropogenic mercury emissions in China. *Atmospheric Environment*, 39(40), 7789–7806.
- Streets, D. G., Horowitz, H. M., Jacob, D. J., Lu, Z., Levin, L., Ter Schure, A. F. H., & Sunderland, E. M. (2017). Total Mercury Released to the Environment by Human Activities. *Environmental Science & Technology*.
- Streets, D. G., Zhang, Q., & Wu, Y. (2009). Projections of global mercury emissions in 2050. *Environmental Science and Technology*, 43(8), 2983–2988.
- Subir, M., Ariya, P. A., & Dastoor, A. P. (2012). A Review of the Sources of Uncertainties in Atmospheric Mercury Modeling II. *Atmospheric Environment*, 46, 1–10.
- Swartz, J. (2016). China's National Emissions Trading System. Tech. rep., International Centre for Trade and Sustainable Development, Geneva, Switzerland.
- Telmer, K., & Veiga, M. (2009). World Emissions of Mercury from Artisanal and Small Scale Gold Mining. In N. Pirrone, & R. Mason (Eds.) *Mercury Fate and Transport in the Global Atmosphere*, chap. 6. Springer.
- Thompson, T. M., Rausch, S., Saari, R. K., & Selin, N. E. (2014). A systems approach to evaluating the air quality co-benefits of US carbon policies. *Nature Climate Change*, 4(10), 917–923.
- Tian, H. Z., Wang, Y., Xue, Z. G., Cheng, K., Qu, Y. P., Chai, F. H., & Hao, J. M. (2010). Trend and characteristics of atmospheric emissions of Hg, As, and Se from coal combustion in China, 1980-2007. *Atmospheric Chemistry and Physics*, 10, 11905–11919.
- Travnikov, O., Angot, H., Artaxo, P., Bencardino, M., Bieser, J., D'Amore, F., Dastoor, A., De Simone, F., Diéguez, M. d. C., Dommergue, A., Ebinghaus, R., Feng, X. B., Gencarelli, C. N., Hedgecock, I. M., Magand, O., Martin, L., Matthias, V., Mashyanov, N., Pirrone, N., Ramachandran, R., Read, K. A., Ryjkov, A., Selin, N. E., Sena, F., Song, S., Sprovieri, F., Wip, D., Wängberg, I., & Yang, X. (2017). Multi-model study of mercury dispersion in the atmosphere: Atmospheric processes and model evaluation. *Atmospheric Chemistry and Physics*, 17, 5271–5295.
- UN General Assembly (2015). *Transforming our world: the 2030 Agenda for Sustainable Development*. 70th session ed.
- UNEP (2013a). *Minamata Convention on Mercury*. United Nations Environment Programme.

- URL <http://www.mercuryconvention.org/Portals/11/documents/Booklets/MinamataConventiononMercury{ }booklet{ }English.pdf>
- UNEP (2013b). *The Global Mercury Assessment*. Geneva, Switzerland: UNEP Chemicals Branch.
URL <http://www.unep.org/PDF/PressReleases/GlobalMercuryAssessment2013.pdf>
- UNEP (2016a). Handbook for the Montreal Protocol on Substances that Deplete the Ozone Layer. Tech. rep., Ozone Secretariat, UNEP.
URL <http://ozone.unep.org/sites/ozone/files/Publications/Handbooks/MP-Handbook-2016-English.pdf>
- UNEP (2016b). Twenty-Eighth Meeting of the Parties to the Montreal Protocol on Substances that Deplete the Ozone Layer, Further Amendment of the Montreal Protocol, UNEP/OzL.Pro.28/CRP/10.
URL <http://conf.montreal-protocol.org/meeting/mop/mop-28/crps/SitePages/Home.aspx>
- UNEP (2017). List of Signatories and Future Parties.
URL <http://www.mercuryconvention.org/Countries>
- UNFCCC (1992). United Nations Framework Convention on Climate Change. Tech. rep., United Nations, New York, New York.
URL <https://unfccc.int/resource/docs/convkp/conveng.pdf>
- UNFCCC (1998). Kyoto Protocol. Tech. rep., United Nations, Kyoto, Japan.
URL <http://unfccc.int/resource/docs/convkp/kpeng.pdf>
- UNFCCC (2015). *Paris Agreement*. Paris: United Nations Framework Convention on Climate Change.
URL <http://unfccc.int/resource/docs/2015/cop21/eng/l09r01.pdf>
- UNFCCC (2017). Paris Agreement - Status of Ratification.
URL <http://unfccc.int/paris{ }agreement/items/9444.php>
- United Nations (2016). Paris Agreement Entry Into Force. Tech. rep.
URL <https://treaties.un.org/doc/Publication/CN/2016/CN.735.2016-Eng.pdf>
- UNU-IHDP, & UNEP (2012). *Inclusive Wealth Report 2012*. New York: Cambridge University Press.
- UNU-IHDP, & UNEP (2014). *Inclusive Wealth Report 2014*. New York: Cambridge University Press.
- US EPA (2014). National Emissions Inventory.
URL <https://www.epa.gov/air-emissions-inventories/national-emissions-inventory-nei>

- van Vuuren, D. P., & Carter, T. R. (2014). Climate and socio-economic scenarios for climate change research and assessment: Reconciling the new with the old. *Climatic Change*, *122*, 415–429.
- Wang, H., & He, J. (2010). The Value of Statistical Life : a Contingent Investigation in China.
URL <https://openknowledge.worldbank.org/handle/10986/3905>
- Wang, L., Wang, S., Zhang, L., Wang, Y., Zhang, Y., Nielsen, C., McElroy, M. B., & Hao, J. (2014). Source apportionment of atmospheric mercury pollution in China using the GEOS-Chem model. *Environmental Pollution*, *190*, 166–175.
- WCED (1987). *Our Common Future*. Oxford; New York: Oxford University Press.
- West, J. J., Fiore, A. M., Horowitz, L. W., & Mauzerall, D. L. (2006). Global Health Benefits of Mitigating Ozone Pollution with Methane Emission Controls. *Proceedings of the National Academy of Sciences of the United States of America*, *103*(11), 3988–3993.
- World Bank (2015). Project Information Document, Capacity Strengthening for Implementation of Minamata Convention on Mercury.
URL <http://documents.worldbank.org/curated/en/967631468019773472/pdf/PID-Print-P151281-08-19-2015-1440030144849.pdf>
- World Bank (2016). Project Appraisal Document on a Proposed Grant to the People’s Republic of China for a Capacity Strengthening for Implementation of Minamata Convention on Mercury Project.
URL <http://documents.worldbank.org/curated/en/179731473645626619/pdf/PAD-after-negotiation-08252016.pdf>
- Wu, Q., Wang, S., Li, G., Liang, S., Lin, C.-J., Wang, Y., Cai, S., Liu, K., & Hao, J. (2016). Temporal trend and spatial distribution of speciated atmospheric mercury emissions in China during 1978–2014. *Environmental Science & Technology*, *50*, 13428–13435.
- Yorifuji, T., Tsuda, T., & Harada, M. (2013). Minamata Disease: a Challenge for Democracy and Justice. In *Late Lessons from Early Warnings: Science, Precaution, Innovation*, chap. 5, (pp. 92–130). Copenhagen: European Environment Agency.
- Zhang, D., Rausch, S., Karplus, V. J., & Zhang, X. (2013). Quantifying regional economic impacts of CO2 intensity targets in China. *Energy Economics*, *40*(2013), 687–701.
URL <http://dx.doi.org/10.1016/j.eneco.2013.08.018>
- Zhang, D., Springmann, M., & Karplus, V. J. (2016a). Equity and emissions trading in China. *Climatic Change*, *134*, 131–146.

- Zhang, L., Wang, S., Hui, M., Zhao, B., & Cai, S. (2016b). Potential of Co-benefit Mercury Control for Coal-Fired Power Plants and Industrial Boilers in China Prepared by . Tech. Rep. February, Natural Resources Defense Council.
URL <https://www.nrdc.org/sites/default/files/co-benefit-mercury-control-report.pdf>
- Zhang, L., Wang, S., Wang, L., Wu, Y., Duan, L., Wu, Q., Wang, F., Yang, M., Yang, H., Hao, J., & Liu, X. (2015). Updated emission inventories for speciated atmospheric mercury from anthropogenic sources in China. *Environmental Science and Technology*, *49*(5), 3185–3194.
- Zhang, Y., Jaeglé, L., van Donkelaar, A., Martin, R. V., Holmes, C. D., Amos, H. M., Wang, Q., Talbot, R., Artz, R., Brooks, S., Luke, W., Holsen, T. M., Felton, D., Miller, E. K., Perry, K. D., Schmeltz, D., Steffen, A., Tordon, R., Weiss-Penzias, P., & Zsolway, R. (2012). Nested-grid simulation of mercury over North America. *Atmospheric Chemistry and Physics*, *12*, 6095–6111.
- Zhao, Y., Zhong, H., Zhang, J., & Nielsen, C. P. (2015). Evaluating the effects of China’s pollution controls on inter-annual trends and uncertainties of atmospheric mercury emissions. *Atmospheric Chemistry and Physics*, *15*, 4317–4337.